Published in final edited form as:
J Hazard Mater. 2021 January 05; 401: 123401. doi:10.1016/j.jhazmat.2020.123401.

Green-synthesized nanocatalysts and nanomaterials for water treatment: Current challenges and future perspectives

Mahmoud Nasrollahzadeh[a,*], **Mohaddeseh Sajjadi**[a], **Siavash Iravani**[b,*], **Rajender S. Varma**[c,d,**]

[a]Department of Chemistry, Faculty of Science, University of Qom, Qom, 37185-359, Iran

[b]Faculty of Pharmacy and Pharmaceutical Sciences, Isfahan University of Medical Sciences, Isfahan, Iran

[c]Chemical Methods and Treatment Branch, Water Infrastructure Division, Center for Environmental Solutions and Emergency Response, U. S. Environmental Protection Agency, 26 West Martin Luther King Drive, Cincinnati, Ohio 45268, USA

[d]Regional Centre of Advanced Technologies and Materials, Palacký University in Olomouc, Šlechtitelů 27, 783 71 Olomouc, Czech Republic

Abstract

Numerous hazardous environmental pollutants in water bodies, both organic and inorganic, have become a critical global issue. As greener and bio-synthesized versions of nanoparticles exhibit significant promise for wastewater treatment, this review discusses trends and future prospects exploiting the sustainable applications of green-synthesized nanocatalysts and nanomaterials for the removal of contaminants and metal ions from aqueous solutions. Recent trends and challenges about these nanocatalysts and nanomaterials and their potential applications in wastewater treatment and water purification are highlighted including toxicity and biosafety issues. This review delineates the pros and cons and critical issues pertaining to the deployment of these nanomaterials endowed with their superior surface area, mechanical properties, significant chemical reactivity, and cost-effectiveness with low energy consumption, for removal of hazardous materials and contaminants from water; comprehensive coverage of these materials for industrial wastewater remediation, and their recovery is underscored by recent advancements in nanofabrication, encompassing intelligent and smart nanomaterials.

Graphical Abstract

[*]Corresponding authors. mahmoudnasr81@gmail.com (M. Nasrollahzadeh), siavashira@gmail.com (S. Iravani). [**]Corresponding author at: Chemical Methods and Treatment Branch, Water Infrastructure Division, Center for Environmental Solutions and Emergency Response, U. S. Environmental Protection Agency, 26 West Martin Luther King Drive, Cincinnati, Ohio 45268, USA. Varma.Rajender@epa.gov (R.S. Varma).

Declaration of Competing Interest

The authors declare that they have no known competing financial interests or personal relationships that could have appeared to influence the work reported in this paper.

Disclaimer

The research presented was not performed or funded by EPA and was not subject to EPA's quality system requirements. The views expressed in this article are those of the author(s) and do not necessarily represent the views or the policies of the U.S. Environmental Protection Agency.

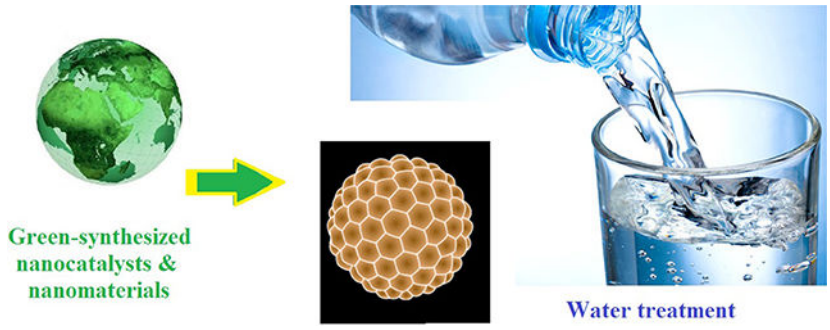

Keywords

Nanocatalysts; Biogenic nanomaterials; Sustainable methods; Green synthesis; Water treatment

1. Introduction

Nano-engineered materials, such as nanoadsorbents, nanometals, nanomembranes, and photocatalysts offer promising options for novel water technologies which can be adapted to customer-specific needs. A large majority of them are compatible with existing treatment technologies and can be integrated simply in the existing set-up. There are numerous contaminants in wastewater discharge which have adverse health effects namely pesticides, textile dyes, plasticizers, disinfection by-products, polychlorinated biphenyls (PCBs), polycyclic aromatic hydrocarbons (PAHs), and emerging pollutants such as perfluorooctanoic acid (PFOA) and perfluorooctane sulfonate (PFOS), endocrine disrupting materials, pharmaceutical and personal care products (Bousselmi et al., 2004; Mozia et al., 2007; Rizzo et al., 2009). Innovative engineered nanomaterials are very encouraging for removal of these hazardous contaminants, as they have high surface areas and remarkable reactivity (Zhang et al., 2019). In this context, the development of greener protocols for the elimination of ionic metal species from water has witnessed profound interest (Iravani, 2011; Shukla and Iravani, 2017; Nadagouda and Varma, 2008; Moulton et al., 2010).

Nanotechnology and nanoscience, an area of research that has a progressed at a very fast pace, present numerous attractive options for water/wastewater treatment. Nowadays, nanostructured materials have garnered attention in the degradation as well as remediation of toxic organic/inorganic pollutants owing to unique physicochemical properties such as their high catalytic activity, high physical/chemical and thermal stability, large specific surface area, significant chemical reactivity, and strong electron transfer ability, among others (Pradhan et al., 2001; Sinha et al., 2013; Xu et al., 2019; Zhang et al., 2014). Indeed, nanomaterials and nanoparticles (NPs) are recently applied to address the environmental issues *e.g.* water contaminant treatment and/or environmental monitoring/sensing; they are considered as an excellent option, since the reactive nanostructures have potential features that render them more efficient to convert and/or remove hazardous/toxic pollutants into toxic-free substances. In general, nanostructured materials *e.g.* nanosorbents, nanoparticles (Pd, Au, Ag, Cu, Fe_3O_4, TiO_2, *etc.*), nanocatalytic membrane systems, are more efficient, require lesser time, environmentally-friendly and constitute low energy approaches but not

all these systems are inexpensive or green, and hence are not applied yet to treat the wastewater on large scales. Consequently, there is an essential need to fabricate some green nanomaterials, which must be very effective, having high activity/efficiency, eco-friendly, green and easy to handle. In this respect, green-fabricated nanomaterials can be considered as good candidates for the photocatalysis application in practical water treatment systems, although still more elaborative studies should be performed regarding the application of these nanomaterials.

Organisms specifically fungi and bacteria are capable of surviving and multiplying under stressful conditions due to the presence of higher concentrations of toxic metals (Beveridge et al., 1996; Rouch et al., 1995). It appears that numerous reducing agents in organisms and biochemical trajectories lead to bioreduction of metal ions. In view of the critical function of these agents, there have been more studies pertaining to the role and appliance of genetically engineered and natural organisms in bioreduction of metal ions (Stephen and Macnaughtont, 1999). It has been realized that many organisms reduce various metals, metalloids and radio nuclides such as uranium(VI) (Lovley et al., 1991; Kashefi and Lovley, 2000; Bansal et al., 2004; Mukherjee et al., 2001; Fredrickson et al., 2000; Lloyd and Macaskie, 2000; Lovley and Phillips, 1992; Lovley et al., 1993) and technetium (VII) (Kashefi and Lovley, 2000; Fredrickson et al., 2000; Lloyd and Macaskie, 2000; Philipse and Maas, 2002; Lloyd and Macaskie, 1996) and trace metals including arsenic(V) (Sweeney et al., 2004; Laverman et al., 1995), chromium(VI) (Kashefi and Lovley, 2000; Fredrickson et al., 2000; Zhang et al., 1998, 1996; Wang, 2000; Lovley, 1993), cobalt(III) (Kashefi and Lovley, 2000; Zhang et al., 1996; Sastry et al., 2003; Slawson et al., 1992; Gorby et al., 1998; Caccavo et al., 1994), manganese(IV) (Kashefi and Lovley, 2000; Lovley, 2000), and selenium (VI) (Konishi et al., 2007; Oremland, 1994); majority of them being hazardous environmental contaminants. Therefore, these organisms can be utilized for removing metal and metal oxides contaminants from water and wastewaters (Lee et al., 2004; Grünberg et al., 2001; Lovley, 1995; Lovley and Coates, 1997). As an example, aquatic macrophytes exhibited great potential for eliminating heavy metals (Sood et al., 2012; Gunawardaha et al., 2016; Sarkar and Jana, 1986) which can be harnessed for producing metallic NPs, as well (Gunawardaha et al., 2016; Korbekandi et al., 2014).

The conventional physicochemical strategies for the fabrication of nanomaterials entail the participation of hazardous and volatile materials. This has prompted the researchers to design suitable bioinspired biogenic and greener strategies which are eco-friendly, safer, and cost-effective for the development of novel and efficient nano-scale adsorbents and catalysts which can be harnessed for eliminating and degrading various contaminants in water (Figs. 1 and 2). Indeed, the presence of various phenolic antioxidants in plants and other microorganisms serve as capping and reducing agents for the production of nanomaterials in varied shapes namely, flowers, wires, rods, and tubes.

In this critical review, current trends and future prospects exploiting the application of green-synthesized nanocatalysts and nanomaterials for water and wastewater treatments are discussed. This encompasses advanced nanomaterials and development of novel nanosorbents attained *via* greener and sustainable processes for removing the contaminants and metal ions from aqueous solutions, including groundwater, drinking water, and

wastewater treatment. Recent trends and forthcoming challenges pertaining to green-synthesized nanocatalysts and nanomaterials and their potential applications for treating and purifying wastewater are highlighted. The development of new ecofriendly treatment methods should be perceived as a critical element for the industries producing hazardous, toxic, and chemically-laden wastewater.

2. Mechanistic aspects

2.1. Mechanism for biological preparation of metal/metal oxide NPs

There are several eco-friendly and biological routes for the biogenic fabrication of nanomaterials using plants and microorganisms (Fig. 3) namely algae, bacteria, fungi, viruses, yeasts, and waste materials or fusion of such biogenic methods with alternative activation means such as microwave and ultrasound (Nasrollahzadeh et al., 2019a; 2019b; Singh et al., 2016). The presence of flavonoids, terpenoids, proteins, vitamins, phenolic acid, glycosides, carbohydrates, polymers, alkaloids and various antioxidants in such sources serve as capping/stabilizing and reducing agents for the production of sustainable nanostructures, namely nanoflowers, nanowires, nanorods, nanotubes, and nanoparticles. The biosynthesis of nanoparticles using plants and microorganisms as living organisms offers several environmental applications (Fig. 2) as exemplified by a simple and eco-friendly protocol deploying *Parthenocissus quinquefolia* leaf extract in presence of oxalic acid for the synthesis Fe, Cu-based nanoparticle adsorbents; they exhibit substantial adsorptive capacity for aqueous Malachite (Zhang et al., 2018).

The historical utilization of organisms in the fabrication of bio (nano)materials dates back to 1980 by Beveridge et al., (Beveridge and Murray, 1980) when they evaluated the synthesis of gold NPs by using the *Bacillus* subtilis as an aerobic, gram-positive bacterium. Indeed, microorganisms have the capability to adsorb and accumulate metal ions, which can secrete a higher amount of enzymes by cell activities, thereby increasing the reduction of metal ions to their elemental form. The microbial generation of NPs depends on the presence of reductive enzymes/metabolites of the cell wall, and either their location on the cell or secretion of soluble enzymes (Fig. 4) (Sengani et al., 2017; Parandhaman et al., 2019; Nair and Pradeep, 2002). Indeed, enzymatic reduction processes have implicated the microbial enzymes/metabolites especially NADH and/or NADPH-dependent enzymatic reduction of metal ions to NPs (Parandhaman et al., 2019; Das et al., 2010).

Das, Marsili et al., (Das et al., 2012) recounted on the biosynthesis mechanism of Au NPs formation in the fungi mycelia of *Rhizopus oryzae*; a sizeable quantities of generated extra- or intracellular enzymes/proteins, apparently play a main function in the reduction of $AuCl_4$– ions to Au NPs and their subsequent stabilization by the capping activity of the enzymes. Consequently, two proteins (42 and 45 kDa) partake in the reduction of gold, whereas alternative protein of 80 kDa serve as capping entity in stabilization of the as-prepared Au NPs. Various enzymes namely nitrate reductase, sulfite reductase, keratinase, and alphaamylase, and also plant macro-enzymes possess the capability to help reduce and stabilize metal ions to NPs (Parandhaman et al., 2019; Durán et al., 2015). In the enzyme-assisted reduction (Durán et al., 2015), different amino acid residues bind to metal/metal oxide ions and then reduce them to metal/metal oxide NPs. These enzymes, secreted from

microorganisms and plants inside or outside of the cell wall, are decidedly suitable for the bulk production of NPs *via* a facile and ecofriendly procedure (Thapa et al., 2017). Owing to the presence of the negative charge-bearing amino acids like glutamic or aspartic acid, the enzymes, peptides and proteins play a vital function in the reduction of metal ions to synthesize NPs. Further, polysaccharides can play a key role in the reduction of metal ions, which are largely available from plants and/or microorganisms; negative surface charge of polysaccharides in view of the presence of carboxylic or phosphoric groups, which can bind with the positively-charged metal/metal oxide ions *via* an electrostatic interactions, culminate in the formation of various metal/metal oxide NPs by the metal ions reduction (Banerjee et al., 2017).

In general, biological/biogenic approaches exploit plant polyphenols, microorganisms, algae, enzymes, and industrial and/or agricultural wastes. Among biomaterials/biomolecules, enzymes and their metabolites (*e.g.,* proteins, polysaccharides, peptide chains, carbohydrates, and nucleic acids, among others) have been utilized as reducing/capping agents for the reduction of metal/metal oxide ions to generate assorted NPs and functionalization of NPs (metal/metal oxides, alloy, *etc.*) on inorganic supports. Coker et al., (Coker et al., 2010) described a novel and environmentally benign approach for the preparation of biogenic magnetite NPs (Fe_3O_4 NPs), and their subsequent decoration with Pd NPs using bacterium *Geobacter sulfurreducens* to reduce Fe^{3+}-oxyhydroxide and Na_2PdCl_4 ions without modifying the surface of bio-mineral. Similarly, Lee et al., (Sureshkumar et al., 2010) synthesized a ferric/ferrous magnetic Ag nanocomposite (PMBC-Ag) as an easily recyclable heterogeneous nanocatalyst deploying bacterial cellulose (BC); Fe_3O_4 NPs gets precipitated, and integrated into the BC nanofibrous structure at alkaline pH, and then coated with a polydopamine layer *via* immersing in a dopamine solution. Subsequently, the PMBC-Ag was fabricated by incorporation of Ag NPs into the dopamine-amended magnetic BC (MBC) nanofiber by the reduction of Ag^+ ions.

Furthermore, biomaterial can serve as an effectual support and host for the NPs. For example, Das et al., (Das et al., 2013) have shown that the cell-free protein extracts of *R. oryzae* can simply be anchored on the nanosilica surface (protein-conjugated nanosilica) and serve as an efficient template and/or host for growth of Ag NPs *in situ* on the nanosilica surface. Indeed, protein-based decoration of Ag NPs on the nanosilica surface (Ag@nanosilica) was accomplished by quickly adsorbing positively-charged Ag^+ ions on the negatively-charged protein surface *via* an electrostatic (π-π stacking) contact. Microscopic studies have revealed that the nanosilica-supported stabilized fungal whole protein performed as both, the reducing and capping agent wherein the spherical Ag NPs (~20 nm) were well-dispersed and stable over the whole surface of nanosilica; they exhibited an enhanced catalytic reduction of the 4-NP by this novel and recoverable Ag@nanosilica.

The biological capacity of plant-mediated synthesis of nanocatalysts and nanomaterials is remarkably enhanced owing to its environmentally benign nature and the unique single-step operation with a mechanism that entails synergistic reduction, stabilization and capping of the NPs. Overall, the mechanism of plant-mediated synthesis of nanomaterials employing diverse plants is presently under continual exploration. Various metal/metal oxide salts,

including chlorides, acetates, and nitrates possess high reduction potentials because metals were attached to acetate and/or halogen and also have an electron donation tendency, which can enhancethe electron density of metals on their conjugative salts. The ionic forms of metals can be easily detached from anionic parts owing to the reduction process, which renders them stable *via* the use of plant extracts (Nasrollahzadeh et al., 2019c, a; Nasrollahzadeh et al., 2020a). For example, a likely mechanism for the Pd NP synthesis *via* the reduction of Pd^{2+} to Pd NPs using plant extract as a reducing/capping agent is presented in Fig. 5; biogenic synthesis of metal NPs using plants is a sustainable technique for generating NPs as shown below:

"Metal salts + Plant sources → Biocompatible metal NPs + Biocompatible by-products"

A generalized view has been proposed for the biosynthesis of metal nanomaterials using the plant biomolecules, such as flavonoids and/or polyphenols for the reduction of the metal ions and the stabilization of the ensuing metal nanomaterials (Fig. 6) (Mittal et al., 2013; Huang et al., 2011a) as exemplified for the reduction/stabilization of $PdCl_2$ using OH groups of *Delonix regia* leaf extract that can reduce Pd(II) to Pd (0) (Fig. 7) (Dauthal and Mukhopadhyay, 2013).

2.2. Mechanistic aspects for the degradation of various contaminants

Various physical, chemical, and biological technologies for treating the wastewater include ion-exchange, reverse osmosis, oxidation, adsorption, flocculation, sedimentation, membrane, ultra-filtration, and advanced oxidation processes (AOPs). Among these conventional technologies applied in pollution control, AOPs, namely the Fenton reaction, photocatalysis, ozonation, and/or combinations of these, are increasingly adopted in the degradation of organic pollutants, due to their great efficiency, easy handling, simplicity, and good reproducibility (Chong et al., 2010; Bremner et al., 2009). AOP includes *in situ* generation of highly reactive and nonselective chemical oxidants (*e.g.* $^{\bullet}OH$, H_2O_2, O_3, $^{\bullet}O_2$) to degrade non-biodegradable and resistant organic contaminants. Indeed, Fenton reaction using $^{\bullet}OH$ radical is a sustainable, effective and low-cost technique for the treatment of water/wastewater, as shown below (Jaafara et al., 2019):

$$\text{“}Fe^{2+} + H_2O_2 + H^{+} \rightarrow Fe^{3+} + \cdot OH + H_2O\text{”}$$

(Jaafar et al. (2019)) have developed a series of quantum calculations based on the DFT (density functional theory) and ELF (electron localization function) for studying the degradation behavior of Neutral Red dye (NR), present in wastewater; mechanism of the Fenton reaction between the NR dye and free radicals ($^{\bullet}OH$) for the degradation of NR dye (Fig. 8) were examined in aqueous medium. An electrophilic/nucleophilic free-radical interaction occurs between the nucleophilic center of NR dye, electrophilic center of hydroxyl radical, oxygen, and nitrogen b (N_b), leading to intermediate (I), which has one of the highest nucleophilic activation at the carbon a (C_a). Then, the second single bond can be formed *via* a nucleophilic attack of the C_a of the NR on the oxygen of the $^{\bullet}OH$ radical leading to intermediate (II). The optimization of the NR dye structure and determination of

global and local descriptors of chemical reactivity (*e.g.* chemical hardness, global/local electrophilicity, global nucleophilicity, chemical potential, and the local nucleophilicity indices) of •OH radical and NR dye were evaluated using the DFT technique.

Numerous pathways such as UV photolysis/photocatalysis, adsorption, reduction and (photo) degradation, have been deployed for treating the contaminants (Fig. 9) and removal organic/inorganic pollutants from groundwater, freshwater sediments, wastewater, *etc* (Eskandarloo et al., 2017).

2.2.1. Photocatalytic degradation of organic pollutants—In general, nanomaterials either adsorb the contaminants or they degrade them by diverse catalytic methods *e.g.* assisted by $NaBH_4$, H_2O_2, and photocatalysis wherein green-synthesized NPs are excellent candidate for the photocatalytic water purification (Fig. 10) (Shivaji et al., 2020); toxic organic contaminants are decomposed into other products (Yaqoob et al., 2020) or complete mineralization of organic contaminants occurs to yield carbon dioxide, water, or some inorganic ions. Generally, a semiconductor *e.g.* TiO_2 would absorb the light that is higher or equal to the semiconductor band gap width, creating electron-hole pairs (e^--h^+). The interaction on the surface of nanocatalyst with adsorbed species takes place in the reduction-oxidation (redox) reactions. Besides, h^+_{vb} react with surface-bound water to form the •OH and concomitantly e^-_{cb} selected using oxygen to generate a superoxide radical anion, as depicted below in equations.

A great deal of effort has recently been expanded to design novel and green photocatalytic materials based on metal-organic frameworks (MOFs), especially suited for their potential utilizations in the green degradation of toxic organic contaminants (Lin and Maggard, 2008; Yu et al., 2005; Liao et al., 2008; Toyao et al., 2013); various reports have appeared on the fabrication of MOF-based (photo)catalysts by transition metals to degrade highly toxic pollutants under visible, UV, or UV/vis light (Yu et al., 2005; Toyao et al., 2013). In this context, a MOF-5 was first suggested to behave as an effective photocatalyst (Fig. 11) (Alvaro et al., 2007); these MOFs possess a wide absorption band located in the range 500–840 nm that are assigned to delocalized electron living on a microsecond time scale, and most likely occupying a conduction band (CB),the actual CB energy value being estimated to be 0.2 V *vs.* NHE, with a 3.4 eV band gap (Fig. 11a). The strategy demonstrated comparable activities for the aqueous phenol degradation to that of a commercial TiO_2 or ZnO (Fig. 11b). As a result, a charge-separation state, with electrons in the CB and holes in valence bands (VB), rendersMOF-5 to function as an effective photocatalyst. Overall, like TiO_2, the phenol photodegradation could be occurring *via* a network of reactions, namely initial generation of radical cations by electron-transfer from phenol to the MOF-5 hole or the formation of oxygen active species (such as superoxide radical anions) *via* the reaction of oxygen with the photo-ejected electrons (Fig. 11c).

In a similar study, (Das et al. (2011)) developed a Zn_4O-containing doubly interpenetrated porous MOF (UTSA-38) with a band gap of 2.85 eV, which revealed good photocatalytic activity for the degradation of methyl orange (MO) in aqueous solutions under dark, visible and UV/vis light. The proposed mechanisms for the photodegradation of MO by UTSA-38

under UV or visible light irradiation are illustrated in Fig. 12; MO can be completely decomposed into colorless small molecules under UV light for 120 min.

2.2.2. Reduction of nitro compounds and dyes—Among different reducing agents, $NaBH_4$ has been extensively considered a favored water soluble reductant and preferred alternative to hydrogen sources in the reduction of toxic nitro compounds to significant and useful amino compounds in an aqueous medium. The $NaBH_4$ activation is a main process, which requires a metal substrate as active site since metal hydride complexes fabricated from the BH_4^- ions *via* π-π stacking interactions have been considered intermediates in this reduction reaction (Nasrollahzadeh et al., 2020b). The reduction of toxic 4-NP using $NaBH_4$ as a reductant was described in presence of Pd nanocatalyst stabilized amine modified zeolite (Pd NPs@Zeo) *via* π-π stacking interactions (Fig. 13) (Nasrollahzadeh et al., 2020b). Pd NPs@Zeo converts $NaBH_4$ to molecular H_2 and also BO_2^- dissociated on the surface nanocatalyst, wherein the adsorbed 4-NP interacts with the dissociated H_2 gas and the 4-NP reduction occurs in a step-wise manner to generate 4-aminophenol. As a result, the as-prepared aminophenol is finally desorbed from the surface of the nanocatalyst and the subsequent catalytic run starts afresh. Indeed, the main role of nanocatalyst is to adsorb the molecular H_2 and/or 4-NP in the close proximity to facilitate simple reduction.

Inspired by the biosynthetic mineralization process, magnetically separable nanobiohybrid catalysts, Fe_3O_4@Ch-AuNPs and Fe_3O_4@Ch-PdNPs (Fig. 14), have been designed and fabricated *via* a three-step procedure (Parandhaman et al., 2016). The spherical Fe_3O_4 NPs (~35 nm) were initially generated using *Shewanella algae* and then functionalized or coated with chitosan, followed by decoration with Pd and/or Au NPs to generate a water dispersible and reusable nanobiohybrid catalyst; they exhibited noteworthy activities for the reduction of 4-NP and photodegradation of dye (> 99 % conversion) in polluted water at room temperature. The reaction was suggested to occur by the adsorption and reduction of MB by Pd or AuNPs through an electron transfer process. The rate of the reactions followed pseudo-second-order rate kinetics; Fe_3O_4@Ch-PdNPs and -AuNPs took just 1 min under UV light to complete the MB reduction with an apparent rate constant (k_{app}) of 5.0 min^{-1} and 4.0 min^{-1}. Besides, authors reported that the normalized rate constant (k_{nor}) values are 1.72×10^2 and 1.14×10^2 $mmol^{-1}s^{-1}$, respectively, representing superior catalytic activities of the synthesized Fe_3O_4@Ch-PdNPs and -AuNPs for the degradation of MB.

2.2.3. Adsorption of arsenic—Green-fabricated amorphous iron NPs (with the specific surface area of 51.1368 m^2 g^{-1}) was evaluated for removing highly toxic and carcinogenic arsenic (As) from polluted resources (Wu et al., 2019). Consequently, it was detected that arsenate was uniformly adsorbed on the surfaces of iron NPs; FTIR evaluation showed that the adsorption was predominantly through an FeOAs bond, while XPS analyses revealed that only As(V) was adsorbed. Thus, the suggested mechanism for arsenate removal is based on primarily iron NPs reacting with arsenate to produce a monodentate chelating ligand and then a bidentate binuclear complex. More investigations demonstrated that the maximum adsorption capacity of the prepared NPs for arsenate was about 14.617 mg g^{-1}, and the optimal pH range for adsorption of anionic arsenate was between 4 and 6 (Wu et al., 2019). The sorption kinetics was also examined, and the Langmuir adsorption isotherms

indicated that As(V) adsorption by iron NPs best fit the regression coefficient (R_L^2 = 0.9903), thus validating the proposed chemisorption; the adsorption efficiency fitted the pseudo-second-order kinetic model well. Thus, the green-synthesis of iron NPs have high application potential towards elimination of As(V) and simplicity of their preparation.

An iron-based MOF, MIL-88B, was green-synthesized at room temperature wherein MIL-88B(Fe), with remarkable adsorption capacity of 156.7 mg g^{-1} at a low dosage, was analyzed for eliminating arsenate in water; capacity for removing trace arsenate on MIL-88B(Fe) was ~32.3 mg g^{-1} at a low equilibrium concentration (6.4 μg L^{-1}), which satisfied the arsenic threshold for drinking water. The FTIR and XPS analyses validated that the arsenate molecules bonded with the oxygen molecules, coordinating with FeO clusters in the framework (Hou et al., 2018).

2.2.4. (Photo)degradation and adsorption of organic contaminants—

Compared with conventional water treatment processes (*e.g.* adsorption, conventional oxidation process, *etc.*), (photo)degradation and Fenton-like reaction have been broadly utilized in the pollutants treatment (Lai et al., 2016; Huang et al., 2017; Wang et al., 2016; Khodadadi et al., 2017a). However, some drawbacks (such as low efficiency/activity, low oxidation rate, low pH levels, *etc.*) restrain the potential applications of these individual approaches to economically dispose the toxic contaminants. As an example, a bio-inspired strategy based on biomimetic photocatalytic systems over a combined g-C_3N_4-imidazole-hemin assisted by H_2O_2 showed excellent photocatalytic oxidation activities under solar irradiation (Chen et al., 2017).

In another study, a low-cost photocatalyst Bi_2WO_6 and an ecofriendly biomimetic material hemin together enabled the development of a novel and efficient hemin-modified Bi_2WO_6 composite *via* a facile solvothermal technique (Yi et al., 2018). Combining experimental and theoretical investigations showed an excellent catalytic activity with enhanced pH tolerance by using simulated-solar light (SSL)/H-Bi_2WO_6/H_2O_2 process. According to the experimental results, a plausible reaction mechanism for high photocatalytic activity/stability of the H-Bi_2WO_6 is suggested in Fig. 15; $^{\bullet}O_2^-$, Fe(IV)=O, and $^{\bullet}$OOH active species played the key role in the SSL/H-Bi_2WO_6/H_2O_2 system for the RhB degradation.

3. Applications of green-synthesized nanomaterials for water and wastewater treatment—

Green-synthesized and biogenic NPs can be explored for remediation in sewage systems, treatment plants, membrane bioreactors and the other state-of-the-art water purification devices to reduce or eliminate the perilous contaminated materials in water resources. However, the size control, stability, aggregation and sedimentation are still persistent challenges for the commercial appliances of biogenic NPs in treatment of effluents. Heavy metals removal and degradation of inorganic, organic, radioactive and pharmaceutical pollutants, nitro compounds (*e.g.* 4-NP as a toxic nitroarene), nitrate, phosphate, and also hazardous dyes such as methyl orange (MO), Congo red (CR), Eosin Y (EY), rhodamine B (RhB), methylene blue (MB), *etc.* have been undertaken *via* nano-adsorbents, nanocatalysts and nano-films in view of their high efficiency and greater surface area (Lapworth et al., 2012; Yadav et al., 2015; Gautam et al.,

2015; Arora et al., 2014; Kim et al., 2007; Gawande and Jenkins-Smith, 2001; Tyagi et al., 2018; Chipasa, 2003).

3.1. Removal of organic and inorganic contaminants

One-step ambient temperature preparation of Au NPs on γ-Al_2O_3 supports (Fig. 16a) has been demonstrated by deploying polyphenols from bayberry tannin (BT) plant (Huang et al., 2011b); formation of Al_2O_3/BT/Au NPs entailed initial reduction of $AuCl_4^-$ by BT as a reducing and stabilizing agent, which up on adsorption and glutaraldehyde-assisted self-crosslinking on the porous γ-Al_2O_3, generated a bridged structure. The activity of well-dispersed spherically-shaped gold NPs on γ-Al_2O_3 with a size of~23 nm (Fig. 16b,c) was revealed for the reduction of 4-NP as an active and recyclable nanocatalyst assisted by $NaBH_4$-mediated reduction.

Biogenic metal NPs from natural sources, such as algae, bacteria, plants and fungi have shown eminent capabilities for environmental applications, especially wastewater treatment. Earth-abundant elements should be considered first in these remediation endeavors. Iron NPs generated using aqueous green tea extract showed catalytic activity to degrade malachite green (Weng et al., 2013; Plachtová et al., 2018; Markova et al., 2014; Nadagouda et al., 2010) and their eco-toxicological impact has been evaluated (Markova et al., 2014). Additionally, the production, characterization and biocompatibility aspects of green tea-derived silver NPs have been reported (Markova et al., 2014). In another study, Anatase TiO_2 NPs doped with iron were produced *via* a greener method by applying aqueous extract of lemongrass (*Cymbopogon citratus*) (Solano et al., 2019), where these Fe-TiO_2 NPs exhibited potential for photocatalytic treatment of wastewater, and degradation of organic pollutants (Solano et al., 2019). Additionally, tea extract-facilitated biofabrication of Fe and Fe/Pd bimetallic NPs (~20−30 nm) has been described for removing trichloroethane, a highly toxic chemical from water *via* reductive degradation mechanism (Smuleac et al., 2011).

The elimination of As(V) and As(III) by deployment of magnetic iron oxide NPs (~5−25 nm) biosynthesized from tea waste has been described (Lunge et al., 2014); the elimination of trivalent and pentavalent arsenic (maximum adsorption capacities were about 188.69 and 153.8 mg g^{-1} for As(III) and As(V), respectively) (Fig. 17) was illustrated (Lunge et al., 2014). Moreover, iron oxide NPs were fabricated by applying bio-reducing agents from eucalyptus extract wherein ensuing NPs were seized in chitosan to form a recyclable magnetic organic-nano iron hybrid for removal of arsenic from water (Martínez-Cabanas et al., 2016).

A reduced graphene oxide-silver NP hybrid nanocomposite was synthesized under greener conditions using aqueous extract of *Brassica nigra* (Karthik et al., 2020) which showed antibacterial activities and could be deployed as a photocatalytic agent for removing dyes; Dye, Direct blue-14 (DB-14) was employed to evaluate the adsorption productivity of the prepared nanocomposites. The unqualified recovery of adsorbent after the reaction and its unchanged efficiency for cyclic applications demonstrated that it may serve as an economically and eco-friendly photocatalyst (Karthik et al., 2020).

Ammonia and phosphate, in natural water resources can make remarkable deterioration of pristine water ecosystems because of eutrophication; thus, the innovative and cost-effective remediation methods are highly necessitated (Xu et al., 2020). In one study, the greener produced iron oxide NPs dispersed onto zeolite by eucalyptus leaf extracts, were applied to concurrently eliminate ammonia and phosphate from aqueous solutions; at primary concentration of 10 mg L^{-1} each for two co-existing ions, the prepared material eliminated 43.3 % of NH_4^+ and 99.8 % of PO_4^{3-}. After optimization evaluations, the conditions for maximum adsorption capacity of the produced material for NH_4^+ and PO_4^{3-} were 3.47 and 38.91 mg g^{-1}, respectively (Xu et al., 2020) (Fig. 18).

In another investigation, water-soluble green-fabricated fluorescent carbon quantum dots (QDs) (~260−400 nm), have been prepared by hydrothermal treatment using *Tamarindus indica* leaves (Bano et al., 2018). The ensuing QDs can be applied as sensitive probe for sensing Hg^{2+} with a detection boundary of 6 nM in the dynamic span of 0 to 0.1 μM; the feasibility of this detecting device was tested by using ‘real’ pond water samples for detection of Hg^{2+}, and may be adaptable for additional analysis (Bano et al., 2018). A large assortment of biosynthesized metallic nanocatalysts deployed for the remediation and degradation of various pollutants in water or wastewater are presented in Tables 1 and 2.

3.2. Removal of pharmaceutical contaminants

Pharmaceutical contaminants, especially antibiotics in the natural water systems, pose different complications and hazardous effects for human health, wherein biogenic nanomaterials can be employed for remediation. For instance, tetracycline, as one of the highest applied antibiotics for human and veterinary applications, can be removed *via* deployment of nano zero-valent technology-based tactic (Yi et al., 2018; Gopal et al., 2020; Yi et al., 2019). The bimetallic nano zero-valent iron (nZVI)-Cu NPs were prepared using pomegranate rind extract for remediation purposes; tetracycline removal of 72 ± 0.5 % (initial tetracycline concentration 10 mg L^{-1}) has been reported with the nZVI-Cu concentration of 750 mg L^{-1} at pH 7. To resolve the colloidal instability and enhance the tetracycline removal, bentonite-supported composite have been employed which displayed remarkable improvement in removal with a considerably decreased NP loading (Fig. 19) (Gopal et al., 2020). In another study, nickel-iron nanocomposite has been ecofriendly fabricated using polyphenol rich pomegranate (*Punica granatum*) peel extract, and ensuing nickel-iron was immobilized on to biocompatible and biodegradable alginate to produce nanocomposite beads (GS-NiFe beads) (Fig. 20) (Ravikumar et al., 2020). By using the optimized conditions (20 mg L^{-1} of tetracycline initial concentration; 1000 mg L^{-1} GS-NiFe concentration in beads; bead weight (wet): 20 % (WV^{-1}); interaction time 90 min), 99 % removal was attained in a batch reactor, with adsorption and degradation processes in the remediation. Additionally, the maximum removal capacity (487 ± 6.84 mg g^{-1}) was obtained under the reaction conditions: bed height: 15 cm; initial tetracycline concentration: 20 mg L^{-1}; and flow rate: 1 mL min^{-1} (Ravikumar et al., 2020).

In an utilization of biogenic nanomaterials, green-synthesized Cu NPs were expeditiously produced using aqueous *Tilia* extract residues (Husein et al., 2019) and the ensuingbiogenic NPs were applied in the removal of three selected pharmaceutical drugs from wastewater

samples; Diclofenac (Dic), Ibuprofen (Ibu), and Naproxen (Nap) could be eliminated 91.4, 74.4, and 86.9 %, respectively with 10.0 mg of Cu NPs at pH 4.5 and 298 k for 60 min. The data fitted well with Langmuir model with R^2, the values of 0.998, 0.998 and 0.977 for Dic, Nap, and Ibu, respectively; the maximum adsorption capacities being 36.0, 33.9, and 33.9 mg g^{-1} for Dic, Nap, and Ibu, respectively. In order to provide useful information on the adsorption kinetic mechanism of non-steroidal anti-inflammatory drugs adsorption onto Cu NPs surface, diverse kinetic models were checked to analyze the kinetic data. Kinetic studies revealed that these sorption processes obeyed the pseudo-second-order model, while the thermodynamic parameters indicated the spontaneous and exothermic and/or physical nature of the adsorption (+38.3, +23.8, and +40.8 kJ mol^{-1} for Dic, Ibu, and Nap, respectively) (Husein et al., 2019).

In yet another attempt, a new Fe_3O_4 nanosorbent was prepared using plant extracts of cucumber (*Cucumis sativus*), lemon (*Citrus limon*), and black grapes (*Vitis vinifera*) *via* a green approach (Stan et al., 2017). The as-prepared Fe_3O_4(cum), Fe_3O_4(lem), and Fe_3O_4(grp) nanosorbents were applied for the elimination of seven antibiotics such as piperacillin, sulfamethoxazole, tetracycline, tazobactam, trimethoprim, erythromycin, and ampicillin from water bodies. The Box-Behnken design method was applied to recognize the optimum conditions for the antibiotics removal; Langmuir, Freundlich, and/or Temkin adsorption isotherm models were the best fitted towards the adsorption of selected antibiotics with an excellent removal of > 90 % was observed for most of these antibiotics.

3.3. Membrane-based water treatment

MOFs have remarkable advantages, including low cost readily achieved raw materials, relatively non-toxic metal source with adequate biocompatibility, and desirable physicochemical characteristics (*e.g.*, semiconductor properties, high porosity and framework flexibility), and thus they can be employed as promising alternatives for environmental remediation (Hou et al., 2018; Lee et al., 2014). Interestingly, a porous matrix membrane (PMM) was constructed using an eco-friendly method, by applying MOF particles as green template, which although is insoluble in polar organic solvents but can be simply washed away by water (Fig. 21) (Lee et al., 2014). Such systems have appliance potential for pressure-driven membranes processes and carbonaceous nano-fiber membranes removing and separating NPs with remarkable selectivity, or osmotically-driven membrane systems, including pressure-retarded osmosis and forward osmosis (Lee et al., 2014).

4. Current challenges and future perspectives

There is a vital need for the introduction of novel advanced water technologies to ensure a high quality of drinking water, with added capacity to eliminate micropollutants. Industrial production processes need to be strengthened *via* the use of flexible and adaptable water treatment systems. One of the most important advantages of nanomaterials, when compared with conventional water technologies, is their ability to integrate various properties, resulting in multifunctional systems such as nanocomposite membranes that enable both, the particle retention and elimination of contaminants. Furthermore, nanomaterials enable higher process efficiency due to their unique characteristics, such as a high surface area. However,

some important drawbacks need to be pointed out at this stage. For instance, materials functionalized with NPs incorporated or deposited on their surface have risk potential, as NPs may be released to the environment where they can get accumulated over a longer period of time. In order to minimize the health risk, several national and international regulations and laws are being established. The main technical limitation of nano-engineered water technologies is that they are seldom adaptable for large-scale processes, and at present, in many cases are not competitive with conventional treatment technologies. Nevertheless, safer and earth-abundant nano-engineered materials offer great potential for innovations in the near future, particularly for the decentralized treatment systems, point-of-use devices, and heavily degradable contaminants. Biogenic NPs are promising materials due to the inherent greenness and sustainability of the production methods, and their good performance in the reduction of environmental contaminants (Gautam et al., 2019). Progress of advanced analytical and imaging technologies has paved various pathways for the assessment and measurement of nano-sized objects, especially for water treatment applications. In view of the applications of hazardous chemicals and materials for producing nano objects, chemical industry has been under stress to subrogate toxic reagents and harmful solvents; the main push has been to deploy biomolecules from organisms as an alternative to damaging synthetic chemicals to produce biocompatible nano objects. It appears that bioprepared nanomaterials can adsorb contaminants from aqueous watercourses or catalyze the degradation of organic pollutants into nontoxic categories. Biogenic nanomaterials are sustainable, relatively inexpensive, can be produced in an energy-efficient manner and ecologically reliable in view of their bio-renewable nature and could play significant roles in decontamination protocols for drinking and industrial wastewaters (Gautam et al., 2019). In terms of deployment of biogenic nanomaterials for water treatment and purification, some important future perspectives need to be considered:

1. The sustainability and toxicity issues need to be evaluated; more elaborative studies are required for application of these green-synthesized nanocatalysts and nanomaterials in industrial and commercial scales. On the other hand, applying nanomaterials may additionally contribute to the secondary pollution, and thus this critical issue should be addressed and evaluated comprehensively.

2. Although the production of these nanomaterials are simple and ecofriendly, some important and challenging aspects should be analyzed and optimized, including the effects of reaction parameters and stability issues, because these factors can modify the behavior of nanomaterials, morphologies and their pollutant removal performance. Further, the purification and extraction of the produced biogenic nanomaterials for additional applications are very important, and they should be isolated with high purity especially in the case of water treatment.

3. Further investigations are needed to find innovative nanohybrids and multifunctional nanomaterials to enhance their effectual usefulness.

4. The cost-effectiveness studies should be addressed to compare the fabrication of green-synthesized nanomaterials with the NPs prepared by conventional approaches.

5. The efficacy issues and evaluation of remedial performances are typically designed on laboratory scales, simulating the variable levels of realistic exposure conditions, but it is crucial to investigate and evaluate the results from realistic environmental conditions.

5. Conclusion

Green-synthesized and biogenic nanocatalysts and nanomaterials can cost-effectively and proficiently eliminate the inorganic, organic, pharmaceutical, and heavy metal pollutants from the aqueous streams. As low cost of production is imperative for their broader applications in wastewater treatment, future studies should be dedicated to refining the economic viability of these nanomaterials and evaluation of their interactive mechanisms in water treatment systems. Additionally, their potential toxicity to human health and the environment need to be thoroughly probed; comprehensive evaluations of their noxiousness are very critical to ensure their safer applications. Further studies are warranted to compare the relative performances of these nanomaterials in terms of energy usage and resource utilization and recognize favorable earth-abundant materials which merit additional developments.

Nanotechnology-facilitated wastewater treatment systems need to ensure not only to circumvent the main challenges encountered by existing technologies but also to tender innovative treatment abilities which can permit economical applications of unconventional water resources to recover and develop for the water supply. Applying green-synthesized nanocatalysts and nanomaterials for the remediation of pollutants and aqueous metal ions are significantly encouraging, but some important and critical issues pertaining to the toxicity and biosafety issues and their mechanistic aspects should be systematically and comprehensively evaluated; more elaborative studies are still demanded to find the low cost, high adsorption capacity, and high selectivity of the fabrication method, as well as the recyclability of green-fabricated nanocatalysts and nanomaterials.

Acknowledgement

The support of the Iranian Nano Council, the University of Qom and Isfahan University of Medical Sciences for this work is greatly appreciated.

References

Adeleke J, Theivasanthi T, Thiruppathi M, Swaminathan M, Akomolafe T, Alabi A, 2018 Photocatalytic degradation of methylene blue by ZnO/NiFe2O4 nanoparticles. Appl. Surf. Sci 455, 195–200.

Aitenneite H, Abboud Y, Tanane O, Solhy A, Sebti S, Bouari AE, 2016 Rapid and green microwave-assisted synthesis of silver nanoparticles using aqueous Phoenix dactylifera L.(Date palm) leaf extract and their catalytic activity for 4-Nitrophenol reduction. J. Mater. Environ. Sci 7, 2335–2339.

Al-Asfar A, Zaheer Z, Aazam ES, 2018 Eco-friendly green synthesis of Ag@ Fe bimetallic nanoparticles: antioxidant, antimicrobial and photocatalytic degradation of bromothymol blue. J. Photochem. Photobiol. B, Biol 185, 143–152.

Ali I, ALOthman ZA, Sanagi MM, 2015 Green synthesis of iron nano-impregnated adsorbent for fast removal of fluoride from water. J. Mol. Liq 211, 457–465.

Ali I, AL-Othman ZA, Alwarthan A, 2016 Green synthesis of functionalized iron nano particles and molecular liquid phase adsorption of ametryn from water. J. Mol. Liq 221, 1168–1174.

Al-Ruqeishi MS, Mohiuddin T, Al-Saadi LK, 2016 Green synthesis of iron oxide nanorods from deciduous Omani mango tree leaves for heavy oil viscosity treatment. Arab. J. Chem

Alvaro M, Carbonell E, Ferrer B, Llabrés i Xamena FX, Garcia H, 2007 Semiconductor behavior of a metal-organic framework (MOF). Chem. Eur. J 13, 5106–5112. [PubMed: 17385196]

Andjelkovic I, Azari S, Erkelens M, Forward P, Lambert MF, Losic D, 2017 Bacterial iron-oxide nanowires from biofilm waste as a new adsorbent for the removal of arsenic from water. RSC Adv. 7, 3941–3948.

Arora PK, Srivastava A, Singh VP, 2014 Bacterial degradation of nitrophenols and their derivatives. J. Hazard. Mater 266, 42–59. [PubMed: 24374564]

Arunachalam R, Dhanasingh S, Kalimuthu B, Uthirappan M, Rose C, Mandal AB, 2012 Phytosynthesis of silver nanoparticles using Coccinia grandis leaf extract and its application in the photocatalytic degradation. Colloids Surf. B Biointerfaces 94, 226–230. [PubMed: 22348986]

Atarod M, Nasrollahzadeh M, Sajadi SM, 2015 Green synthesis of a Cu/reduced graphene oxide/Fe_3O_4 nanocomposite using Euphorbia wallichii leaf extract and its application as a recyclable and heterogeneous catalyst for the reduction of 4-nitrophenol and rhodamine B. RSC Adv. 5, 91532–91543.

Ayodhya D, Veerabhadram G, 2017 Preparation, characterization, photocatalytic, sensing and antimicrobial studies of Calotropis gigantea leaf extract capped CuS NPs by a green approach. J. Inorg. Organomet. Polym. Mater 27, 215–230.

Banerjee A, Halder U, Bandopadhyay R, 2017 Preparations and applications of polysaccharide based green synthesized metal nanoparticles: a state-of-the-art. J. Clust. Sci 28, 1803–1813.

Bano D, Kumar V, Singha VK, Hasan SH, 2018 Green synthesis of fluorescent carbon quantum dots for the detection of mercury(II) and glutathione. New J. Chem 42, 5814–5821.

Bansal V, Rautaray D, Ahmad A, Sastry M, 2004 Biosynthesis of zirconia nanoparticles using the fungus Fusarium oxysporum. J. Mater. Chem 14, 3303–3305.

Beveridge T, Murray R, 1980 Sites of metal deposition in the cell wall of Bacillus subtilis. J. Bacteriol 141, 876–887. [PubMed: 6767692]

Beveridge T, Hughes M, Lee H, Leung K, Poole R, Savvaidis I, Silver S, Trevors J, 1996 Metal-microbe interactions: contemporary approaches Advances in Microbial Physiology. Elsevier, pp. 177–243.

Bonigala B, Kasukurthi B, Konduri VV, Mangamuri UK, Gorrepati R, Poda S, 2018 Green synthesis of silver and gold nanoparticles using Stemona tuberosa Lour and screening for their catalytic activity in the degradation of toxic chemicals. Environ. Sci. Pollut. Res. Int 25, 32540–32548. [PubMed: 30238263]

Bordbar M, 2017 Biosynthesis of Ag/almond shell nanocomposite as a cost-effective and efficient catalyst for degradation of 4-nitrophenol and organic dyes. RSC Adv. 7, 180–189.

Bordbar M, Mortazavimanesh N, 2017 Green synthesis of Pd/walnut shell nanocomposite using Equisetum arvense L. Leaf extract and its application for the reduction of 4-nitrophenol and organic dyes in a very short time. Environ. Sci. Pollut. Res. Int 24, 4093–4104. [PubMed: 27933496]

Bordbar M, Sharifi-Zarchi Z, Khodadadi B, 2017 Green synthesis of copper oxide nanoparticles/clinoptilolite using Rheum palmatum L. Root extract: high catalytic activity for reduction of 4-nitro phenol, rhodamine B, and methylene blue. J. Solgel Sci. Technol 81, 724–733.

Bordbar M, Negahdar N, Nasrollahzadeh M, 2018 Melissa Officinalis L. Leaf extract assisted green synthesis of CuO/ZnO nanocomposite for the reduction of 4-nitrophenol and Rhodamine B. Sep. Purif. Technol 191, 295–300.

Bousselmi L, Geissen S-U, Schroeder H, 2004 Textile wastewater treatment and reuse by solar catalysis: results from a pilot plant in Tunisia. Water Sci. Technol 49, 331–337. [PubMed: 15077992]

Bremner DH, Molina R, Martínez F, Melero JA, Segura Y, 2009 Degradation of phenolic aqueous solutions by high frequency sono-Fenton systems (US–Fe2O3/SBA-15–H2O2). Appl. Catal. B 90, 380–388.

Caccavo F, Lonergan DJ, Lovley DR, Davis M, Stolz JF, McInerney MJ, 1994 Geobacter sulfurreducens sp. nov., a hydrogen-and acetate-oxidizing dissimilatory metal-reducing microorganism. Appl. Environ. Microbiol 60, 3752–3759. [PubMed: 7527204]

Cao D, Jin X, Gan L, Wang T, Chen Z, 2016 Removal of phosphate using iron oxide nanoparticles synthesized by eucalyptus leaf extract in the presence of CTAB surfactant. Chemosphere 159, 23–31. [PubMed: 27268791]

Chen X, Lu W, Xu T, Li N, Qin D, Zhu Z, Wang G, Chen W, 2017 A bio-inspired strategy to enhance the photocatalytic performance of g-C3N4 under solar irradiation by axial coordination with hemin. Appl. Catal. B 201, 518–526.

Chipasa KB, 2003 Accumulation and fate of selected heavy metals in a biological wastewater treatment system. Waste Manag. 23, 135–143. [PubMed: 12623088]

Chong MN, Jin B, Chow CWK, Saint C, 2010 Recent developments in photocatalytic water treatment technology: a review. Water Res. 44, 2997–3027. [PubMed: 20378145]

Chowdhury IH, Ghosh S, Naskar MK, 2016 Aqueous-based synthesis of mesoporous TiO2 and Ag–TiO2 nanopowders for efficient photodegradation of methylene blue. Ceram. Int 42, 2488–2496.

Coker VS, Bennett JA, Telling ND, Henkel T, Charnock JM, van der Laan G, Pattrick RA, Pearce CI, Cutting RS, Shannon IJ, 2010 Microbial engineering of nanoheterostructures: biological synthesis of a magnetically recoverable palladium nanocatalyst. ACS Nano 4, 2577–2584. [PubMed: 20394356]

Das SK, Das AR, Guha AK, 2010 Microbial synthesis of multishaped gold nanostructures. Small 6, 1012–1021. [PubMed: 20376859]

Das MC, Xu H, Wang Z, Srinivas G, Zhou W, Yue Y-F, Nesterov VN, Qian G, Chen B, 2011 A Zn 4 O-containing doubly interpenetrated porous metal–organic framework for photocatalytic decomposition of methyl orange. Chem. Commun 47, 11715–11717.

Das SK, Liang J, Schmidt M, Laffir F, Marsili E, 2012 Biomineralization mechanism of gold by zygomycete fungi Rhizopous oryzae. ACS Nano 6, 6165–6173. [PubMed: 22708541]

Das SK, Khan MMR, Guha AK, Naskar N, 2013 Bio-inspired fabrication of silver nanoparticles on nanostructured silica: characterization and application as a highly efficient hydrogenation catalyst. Green Chem. 15, 2548–2557.

Dauthal P, Mukhopadhyay M, 2013 Biosynthesis of palladium nanoparticles using Delonix regia leaf extract and its catalytic activity for nitro-aromatics hydrogenation. Ind. Eng. Chem. Res 52, 18131–18139.

Dauthal P, Mukhopadhyay M, 2015 Agro-industrial waste-mediated synthesis and characterization of gold and silver nanoparticles and their catalytic activity for 4-nitroaniline hydrogenation. Korean J. Chem. Eng 32, 837–844.

Dauthal P, Mukhopadhyay M, 2016 AuPd bimetallic nanoparticles: single step biofabrication, structural characterization and catalytic activity. J. Ind. Eng. Chem 35, 45–53.

De Corte S, Sabbe T, Hennebel T, Vanhaecke L, De Gusseme B, Verstraete W, Boon N, 2012 Doping of biogenic Pd catalysts with Au enables dechlorination of diclofenac at environmental conditions. Water Res. 46, 2718–2726. [PubMed: 22406286]

De Gusseme B, Hennebel T, Vanhaecke L, Soetaert M, Desloover J, Wille K, Verbeken K, Verstraete W, Boon N, 2011 Biogenic palladium enhances diatrizoate removal from hospital wastewater in a microbial electrolysis cell. Environ. Sci. Technol 45, 5737–5745. [PubMed: 21663047]

Devi TB, Ahmaruzzaman M, 2016 Bio-inspired sustainable and green synthesis of plasmonic Ag/AgCl nanoparticles for enhanced degradation of organic compound from aqueous phase. Environ. Sci. Pollut. Res. Int 23, 17702–17714. [PubMed: 27246560]

Devi TB, Ahmaruzzaman M, 2017 Bio-inspired facile and green fabrication of Au@ Ag@ AgCl core–double shells nanoparticles and their potential applications for elimination of toxic emerging pollutants: a green and efficient approach for wastewater treatment. Chem. Eng. J 317, 726–741.

Devi TB, Begum S, Ahmaruzzaman M, 2016 Photo-catalytic activity of Plasmonic Ag@ AgCl nanoparticles (synthesized via a green route) for the effective degradation of Victoria blue B from aqueous phase. J. Photochem. Photobiol. B, Biol 160, 260–270.

Dinda G, Halder D, Mitra A, Pal N, Vázquez-Vázquez C, López-Quintela MA, 2017 Study of the antibacterial and catalytic activity of silver colloids synthesized using the fruit of Sapindus mukorossi. New J. Chem 41, 10703–10711.

Durán M, Silveira CP, Durán N, 2015 Catalytic role of traditional enzymes for biosynthesis of biogenic metallic nanoparticles: a mini-review. IET Nanobiotechnol. 9, 314–323. [PubMed: 26435286]

Ehrampoush MH, Miria M, Salmani MH, Mahvi AH, 2015 Cadmium removal from aqueous solution by green synthesis iron oxide nanoparticles with tangerine peel extract. J. Environ. Health Sci. Eng 13, 84. [PubMed: 26682059]

Eskandarloo H, Kierulf A, Abbaspourrad A, 2017 Nano-and micromotors for cleaning polluted waters: focused review on pollutant removal mechanisms. Nanoscale 9, 13850–13863. [PubMed: 28920114]

Farhadi S, Ajerloo B, Mohammadi A, 2017 Green biosynthesis of spherical silver nanoparticles by using date palm (phoenix dactylifera) fruit extract and study of their antibacterial and catalytic activities. Acta Chim. Slov 64, 129–143. [PubMed: 28380222]

Fredrickson JK, Kostandarithes HM, Li S, Plymale AE, Daly M, 2000 Reduction of fe (III), cr (VI), U (VI), and tc (VII) byDeinococcus radiodurans R1. Appl. Environ. Microbiol 66, 2006–2011. [PubMed: 10788374]

Gan L, Lu Z, Cao D, Chen Z, 2018 Effects of cetyltrimethylammonium bromide on the morphology of green synthesized Fe3O4 nanoparticles used to remove phosphate. Mater. Sci. Eng C 82, 41–45.

Ganesh M, Lee SG, Jayaprakash J, Mohankumar M, Jang HT, 2019 Hydnocarpus alpina Wt extract mediated green synthesis of ZnO nanoparticle and screening of its anti-microbial, free radical scavenging, and photocatalytic activity. Biocatal. Agric. Biotechnol 19, 101129.

Garai C, Hasan SN, Barai AC, Ghorai S, Panja SK, Bag BG, 2018 Green synthesis of Terminalia arjuna-conjugated palladium nanoparticles (TA-PdNPs) and its catalytic applications. J. Nanostructure Chem 8, 465–472.

Garole V, Choudhary B, Tetgure S, Garole D, Borse A, 2019 Palladium nanocatalyst: green synthesis, characterization, and catalytic application. Int. J. Environ. Sci. Technol 1–8.

Gautam PK, Gautam RK, Banerjee S, Lofrano G, Sanroman MA, Chattopadhyaya MC, Pandey J, 2015 Preparation of activated carbon from Alligator weed (Alternenthera philoxeroids) and its application for tartrazine removal: Isotherm, kinetics and spectroscopic analysis. J. Environ. Chem. Eng 3, 2560–2568.

Gautam PK, Singh A, Misra K, Sahoo AK, Samanta SK, 2019 Synthesis and applications of biogenic nanomaterials in drinking and wastewater treatment. J. Environ. Manage 231, 734–748. [PubMed: 30408767]

Gawande K, Jenkins-Smith H, 2001 Nuclear waste transport and residential property values: estimating the effects of perceived risks. J. Environ. Econ. Manage 42, 207–233.

Gnanaprakasam P, Selvaraju T, 2014 Green synthesis of self assembled silver nanowire decorated reduced graphene oxide for efficient nitroarene reduction. RSC Adv. 4, 24518–24525.

Gopal G, Sankar H, Natarajan C, Mukherjee A, 2020 Tetracycline removal using green synthesized bimetallic nZVI-Cu and bentonite supported green nZVI-Cu nanocomposite: a comparative study. J. Environ. Manage 254, 109812. [PubMed: 31733482]

Gopalakrishnan R, Loganathan B, Raghu K, 2015 Green synthesis of Au–Ag bimetallic nanocomposites using Silybum marianum seed extract and their application as a catalyst. RSC Adv. 5, 31691–31699.

Gorby YA, Caccavo F, Bolton H, 1998 Microbial reduction of cobaltIIIEDTA-in the presence and absence of manganese (IV) oxide. Environ. Sci. Technol 32, 244–250.

Grünberg K, Wawer C, Tebo BM, Schüler D, 2001 A large gene cluster encoding several magnetosome proteins is conserved in different species of magnetotactic bacteria. Appl. Environ. Microbiol 67, 4573–4582. [PubMed: 11571158]

Gunawardaha D, Malkanthi L, Bandara N, 2016 A study on the Phytoremediation Potential of Azolla pinnata under laboratory conditions. J. Tropic. Forestry Environ 6 (01), 36–49.

Gurushantha K, Anantharaju K, Nagabhushana H, Sharma S, Vidya Y, Shivakumara C, Nagaswarupa H, Prashantha S, Anilkumar M, 2015 Facile green fabrication of iron-doped cubic ZrO2

nanoparticles by Phyllanthus acidus: structural, photocatalytic and photoluminescent properties. J. Mol. Catal. A Chem 397, 36–47.

Gurushantha K, Anantharaju K, Renuka L, Sharma S, Nagaswarupa H, Prashantha S, Vidya Y, Nagabhushana H, 2017 New green synthesized reduced graphene oxide–ZrO 2 composite as high performance photocatalyst under sunlight. RSC Adv. 7, 12690–12703.

Harshiny M, Iswarya CN, Matheswaran M, 2015 Biogenic synthesis of iron nanoparticles using Amaranthus dubius leaf extract as a reducing agent. Powder Technol. 286, 744–749.

Hashemi Salehi M, Yousefi M, Hekmati M, Balali E, 2019 Application of palladium nanoparticle-decorated Artemisia abrotanum extract-modified graphene oxide for highly active catalytic reduction of methylene blue, methyl orange and rhodamine B. Appl. Organomet. Chem 33, e5123.

Hatamifard A, Nasrollahzadeh M, Lipkowski J, 2015 Green synthesis of a natrolite zeolite/palladium nanocomposite and its application as a reusable catalyst for the reduction of organic dyes in a very short time. RSC Adv. 5, 91372–91381.

Hatamifard A, Nasrollahzadeh M, Sajadi SM, 2016 Biosynthesis, characterization and catalytic activity of an Ag/zeolite nanocomposite for base-and ligand-free oxidative hydroxylation of phenylboronic acid and reduction of a variety of dyes at room temperature. New J. Chem 40, 2501–2513.

Hazarika M, Borah D, Bora P, Silva AR, Das P, 2017 Biogenic synthesis of palladium nanoparticles and their applications as catalyst and antimicrobial agent. PLoS One 12, e0184936. [PubMed: 28957342]

Hoag GE, Collins JB, Holcomb JL, Hoag JR, Nadagouda MN, Varma RS, 2009 Degradation of bromothymol blue by ‘greener’nano-scale zero-valent iron synthesized using tea polyphenols. J. Mater. Chem 19, 8671–8677.

Hou S, Wu Y. n., Feng L, Chen W, Wang Y, Morlay C, Li F, 2018 Green synthesis and evaluation of an iron-based metal–organic framework MIL-88B for efficient decontamination of arsenate from water. Dalton Trans. 47, 2222–2231. [PubMed: 29363689]

Huang J, Zhan G, Zheng B, Sun D, Lu F, Lin Y, Chen H, Zheng Z, Zheng Y, Li Q, 2011a Biogenic silver nanoparticles by Cacumen platycladi extract: synthesis, formation mechanism, and antibacterial activity. Ind. Eng. Chem. Res 50, 9095–9106.

Huang X, Liao X, Shi B, 2011b Synthesis of highly active and reusable supported gold nanoparticles and their catalytic applications to 4-nitrophenol reduction. Green Chem. 13, 2801–2805.

Huang L, Weng X, Chen Z, Megharaj M, Naidu R, 2014a Green synthesis of iron nanoparticles by various tea extracts: comparative study of the reactivity. Spectrochim. Acta A. Mol. Biomol. Spectrosc 130, 295–301. [PubMed: 24793479]

Huang L, Weng X, Chen Z, Megharaj M, Naidu R, 2014b Synthesis of iron-based nanoparticles using oolong tea extract for the degradation of malachite green. Spectrochim. Acta A. Mol. Biomol. Spectrosc 117, 801–804. [PubMed: 24094918]

Huang L, Luo F, Chen Z, Megharaj M, Naidu R, 2015 Green synthesized conditions impacting on the reactivity of Fe NPs for the degradation of malachite green. Spectrochim. Acta A 137, 154–159.

Huang D, Hu C, Zeng G, Cheng M, Xu P, Gong X, Wang R, Xue W, 2017 Combination of Fenton processes and biotreatment for wastewater treatment and soil remediation. Sci. Total Environ 574, 1599–1610. [PubMed: 27608610]

Huo C, Khoshnamvand M, Liu P, Yuan C-G, Cao W, 2018 Eco-friendly approach for biosynthesis of silver nanoparticles using Citrus maxima peel extract and their characterization, catalytic, antioxidant and antimicrobial characteristics. Mater. Res. Express 6, 015010.

Husein DZ, Hassanien R, Al-Hakkani MF, 2019 Green-synthesized copper nanoadsorbent for the removal of pharmaceutical pollutants from real wastewater samples. Heliyon 5, e02339. [PubMed: 31485528]

Ijaz F, Shahid S, Khan SA, Ahmad W, Zaman S, 2017 Green synthesis of copper oxide nanoparticles using Abutilon indicum leaf extract: antimicrobial, antioxidant and photocatalytic dye degradation activitie. Trop. J. Pharm. Res 16, 743–753.

Iravani S, 2011 Green synthesis of metal nanoparticles using plants. Green Chem. 13, 2638–2650.

Jaafar A, El Ayouchia HB, Lakbaibi Z, Boussaoud A, Jodeh S, Azzaoui K, Tabyaoui M, 2019 Degradation of pollutant dye in aqueous solution using Fenton reaction: a DFT study. GP Globalize Res. J. Chem 2 (1), 53–61.

Jaafara A, Driouichb A, Lakbaibib Z, El Ayouchiac HB, Azzaouid K, Boussaouda A, Jodehe S, 2019 Central composite design for the optimization of Basic Red V degradation in aqueous solution using Fenton reaction. Desalin. Water Treat 158, 364–371.

Jafarirad S, Rasoulpour I, Divband B, Hammami Torghabe I, Kosari-Nasab M, 2018 Innovative biocapped CuO nano-photocatalysts: a rapid and green method for photocatalytic degradation of 4-nitrophenol. Mater. Res. Innov 22, 415–421.

Jain R, Jordan N, Schild D, Van Hullebusch ED, Weiss S, Franzen C, Farges F, Hübner R, Lens PN, 2015 Adsorption of zinc by biogenic elemental selenium nanoparticles. Chem. Eng. J 260, 855–863.

Jiang Z, Liu D, Jiang D, Wei W, Qian K, Chen M, Xie J, 2014 Bamboo leafassisted formation of carbon/nitrogen co-doped anatase TiO 2 modified with silver and graphitic carbon nitride: novel and green synthesis and cooperative photocatalytic activity. J. Chem. Soc. Dalton Trans 43, 13792–13802.

Kaliraj L, Ahn JC, Rupa EJ, Abid S, Lu J, Yang DC, 2019 Synthesis of panos extract mediated ZnO nano-flowers as photocatalyst for industrial dye degradation by UV illumination. J. Photochem. Photobiol. B, Biol 199, 111588.

Kalpana V, Rajeswari VD, 2018 Synthesis of palladium nanoparticles via a green route using Lagenaria siceraria: assessment of their innate antidandruff, insecticidal and degradation activities. Mater. Res. Express 5, 115406.

Kalpana V, Chakraborthy P, Palanichamy V, Rajeswari VD, 2016 Synthesis and characterization of copper nanoparticles using Tridax procumbens and its application in degradation of bismarck brown. Analysis 10, 17.

Kandasamy R, 2017 A novel single step synthesis and surface functionalization of iron oxide magnetic nanoparticles and thereof for the copper removal from pigment industry effluent. Sep. Purif. Technol 188, 458–467.

Karthiga Devi G, Senthil Kumar P, Sathish Kumar K, 2016 Green synthesis of novel silver nanocomposite hydrogel based on sodium alginate as an efficient biosorbent for the dye wastewater treatment: prediction of isotherm and kinetic parameters. Desalin. Water Treat 57, 27686–27699.

Karthik C, Swathi N, Pandi Prabha S, Caroline DG, 2020 Green synthesized rGOAgNP hybrid nanocomposite – an effective antibacterial adsorbent for photocatalytic removal of DB-14 dye from aqueous solution. J. Environ. Chem. Eng 8, 103577.

Karthika V, Arumugam A, Gopinath K, Kaleeswarran P, Govindarajan M, Alharbi NS, Kadaikunnan S, Khaled JM, Benelli G, 2017 Guazuma ulmifolia barksynthesized Ag, Au and Ag/Au alloy nanoparticles: photocatalytic potential, DNA/protein interactions, anticancer activity and toxicity against 14 species of microbial pathogens. J. Photochem. Photobiol. B, Biol 167, 189–199.

Kashefi K, Lovley DR, 2000 Reduction of Fe (III), Mn (IV), and toxic metals at 100 C by Pyrobaculum islandicum. Appl. Environ. Microbiol 66, 1050–1056. [PubMed: 10698770]

Katata-Seru L, Moremedi T, Aremu OS, Bahadur I, 2018 Green synthesis of iron nanoparticles using Moringa oleifera extracts and their applications: removal of nitrate from water and antibacterial activity against Escherichia coli. J. Mol. Liq 256, 296–304.

Kathiravan V, 2018 Green synthesis of silver nanoparticles using different volumes of Trichodesma indicum leaf extract and their antibacterial and photocatalytic activities. Res. Chem. Intermed 44, 4999–5012.

Kaviya S, Prasad E, 2015 Biogenic synthesis of ZnO–Ag nano custard apples for efficient photocatalytic degradation of methylene blue by sunlight irradiation. RSC Adv. 5, 17179–17185.

Khan ZUH, Khan A, Shah A, Wan P, Chen Y, Khan GM, Khan AU, Tahir K, Muhammad N, Khan HU, 2016 Enhanced photocatalytic and electrocatalytic applications of green synthesized silver nanoparticles. J. Mol. Liq 220, 248–257.

Khan SA, Noreen F, Kanwal S, Iqbal A, Hussain G, 2018 Green synthesis of ZnO and Cu-doped ZnO nanoparticles from leaf extracts of Abutilon indicum, Clerodendrum infortunatum, Clerodendrum

inerme and investigation of their biological and photocatalytic activities. Mater. Sci. Eng C 82, 46–59.

Khan ZUH, Sadiq HM, Shah NS, Khan AU, Muhammad N, Hassan SU, Tahir K, Khan FU, Imran M, Ahmad N, 2019 Greener synthesis of zinc oxide nanoparticles using Trianthema portulacastrum extract and evaluation of its photocatalytic and biological applications. J. Photochem. Photobiol. B, Biol 192, 147–157.

Khodadadi B, Bordbar M, Nasrollahzadeh M, 2017a Achillea millefolium L. Extract mediated green synthesis of waste peach kernel shell supported silver nanoparticles: application of the nanoparticles for catalytic reduction of a variety of dyes in water. J. Colloid Interface Sci 493, 85–93. [PubMed: 28088570]

Khodadadi B, Bordbar M, Yeganeh-Faal A, Nasrollahzadeh M, 2017b Green synthesis of Ag nanoparticles/clinoptilolite using Vaccinium macrocarpon fruit extract and its excellent catalytic activity for reduction of organic dyes. J. Alloys. Compd 719, 82–88.

Khoshnamvand M, Huo C, Liu J, 2019 Silver nanoparticles synthesized using Allium ampeloprasum L. Leaf extract: characterization and performance in catalytic reduction of 4-nitrophenol and antioxidant activity. J. Mol. Struct 1175, 90–96.

Kim SD, Cho J, Kim IS, Vanderford BJ, Snyder SA, 2007 Occurrence and removal of pharmaceuticals and endocrine disruptors in South Korean surface, drinking, and waste waters. Water Res. 41, 1013–1021. [PubMed: 16934312]

Konishi Y, Tsukiyama T, Tachimi T, Saitoh N, Nomura T, Nagamine S, 2007 Microbial deposition of gold nanoparticles by the metal-reducing bacterium Shewanella algae. Electrochim. Acta 53, 186–192.

Kora AJ, Rastogi L, 2018 Green synthesis of palladium nanoparticles using gum ghatti (Anogeissus latifolia) and its application as an antioxidant and catalyst. Arab. J. Chem 11, 1097–1106.

Korbekandi H, Chitsazi MR, Asghari G, Najafi RB, Badii A, Iravani S, 2014 Green biosynthesis of silver nanoparticles using Azolla pinnata whole plant hydroalcoholic extract. Green Process. Synth 3, 365–373.

Kuang Y, Wang Q, Chen Z, Megharaj M, Naidu R, 2013 Heterogeneous Fenton-like oxidation of monochlorobenzene using green synthesis of iron nanoparticles. J. Colloid Interface Sci 410, 67–73. [PubMed: 24034218]

Kumar B, Smita K, Cumbal L, Debut A, 2015 Ultrasound agitated phytofabrication of palladium nanoparticles using Andean blackberry leaf and its photocatalytic activity. J. Saudi Chem. Soc 19, 574–580.

Kumar B, Smita K, Angulo Y, Cumbal L, 2016a Valorization of rambutan peel for the synthesis of silver-doped titanium dioxide (Ag/TiO2) nanoparticles. Green Process. Synth 5, 371–377.

Kumar B, Smita K, Cumbal L, 2016b Biosynthesis of silver nanoparticles using lavender leaf and their applications for catalytic, sensing, and antioxidant activities. Nanotechnol. Rev 5, 521–528.

Kumar B, Vizuete KS, Sharma V, Debut A, Cumbal L, 2019 Ecofriendly synthesis of monodispersed silver nanoparticles using Andean Mortiño berry as reductant and its photocatalytic activity. Vacuum 160, 272–278.

Lai C, Wang M-M, Zeng G-M, Liu Y-G, Huang D-L, Zhang C, Wang R-Z, Xu P, Cheng M, Huang C, 2016 Synthesis of surface molecular imprinted TiO2/graphene photocatalyst and its highly efficient photocatalytic degradation of target pollutant under visible light irradiation. Appl. Surf. Sci 390, 368–376.

Lapworth D, Baran N, Stuart M, Ward R, 2012 Emerging organic contaminants in groundwater: a review of sources, fate and occurrence. Environ. Pollut 163, 287–303. [PubMed: 22306910]

Lateef A, Akande MA, Ojo SA, Folarin BI, Gueguim-Kana EB, Beukes LS, 2016 Paper wasp nest-mediated biosynthesis of silver nanoparticles for antimicrobial, catalytic, anticoagulant, and thrombolytic applications. 3 Biotech 6, 140.

Laverman AM, Blum JS, Schaefer JK, Phillips E, Lovley DR, Oremland RS, 1995 Growth of strain SES-3 with arsenate and other diverse electron acceptors. Appl. Environ. Microbiol 61, 3556–3561. [PubMed: 16535143]

Lee H, Purdon AM, Chu V, Westervelt RM, 2004 Controlled assembly of magnetic nanoparticles from magnetotactic bacteria using microelectromagnets arrays. Nano Lett. 4, 995–998.

Lee JY, Tang CY, Huo F, 2014 Fabrication of porous matrix membrane (PMM) using metal-organic framework as green template for water treatment. Sci. Rep 4, 3740. [PubMed: 24435326]

Liao Z-L, Li G-D, Bi M-H, Chen J-S, 2008 Preparation, structures, and photocatalytic properties of three new uranyl– organic assembly compounds. Inorg. Chem 47, 4844–4853. [PubMed: 18447330]

Lin H, Maggard PA, 2008 Synthesis and structures of a new series of silver-vanadate hybrid solids and their optical and photocatalytic properties. Inorg. Chem 47, 8044–8052. [PubMed: 18698760]

Lingamdinne LP, Chang Y-Y, Yang J-K, Singh J, Choi E-H, Shiratani M, Koduru JR, Attri P, 2017 Biogenic reductive preparation of magnetic inverse spinel iron oxide nanoparticles for the adsorption removal of heavy metals. Chem. Eng. J 307, 74–84.

Lloyd J, Macaskie L, 1996 A novel PhosphorImager-Based technique for monitoring the microbial reduction of technetium. Appl. Environ. Microbiol 62, 578–582. [PubMed: 16535242]

Lloyd JR, Macaskie LE, 2000 Bioremediation of radionuclide-containing wastewaters, in: environmental microbe-metal interactions. Abstr. Gen. Meet. Am. Soc. Microbiol 277–327.

Lopez-Miranda JL, González MV, Mares-Briones F, Cervantes-Chávez J, Esparza R, Rosas G, Pérez R, 2018 Catalytic and antibacterial evaluation of silver nanoparticles synthesized by a green approach. Res. Chem. Intermed 44, 7479–7490.

Lovley DR, 1993 Dissimilatory metal reduction. Annu. Rev. Microbiol 47, 263–290. [PubMed: 8257100]

Lovley DR, 1995 Bioremediation of organic and metal contaminants with dissimilatory metal reduction. J. Ind. Microbiol 14, 85–93. [PubMed: 7766214]

Lovley DR, 2000 Fe (III) and Mn (IV) reduction, in: environmental microbe-metal interactions. Abstr. Gen. Meet. Am. Soc. Microbiol 3–30.

Lovley DR, Coates JD, 1997 Bioremediation of metal contamination. Curr. Opin. Biotechnol 8, 285–289. [PubMed: 9206008]

Lovley DR, Phillips EJ, 1992 Bioremediation of uranium contamination with enzymatic uranium reduction. Environ. Sci. Technol 26, 2228–2234.

Lovley DR, Phillips EJ, Gorby YA, Landa ER, 1991 Microbial reduction of uranium. Nature 350, 413.

Lovley DR, Roden EE, Phillips E, Woodward J, 1993 Enzymatic iron and uranium reduction by sulfate-reducing bacteria. Mar. Geol 113, 41–53.

Lunge S, Singh S, Sinha A, 2014 Magnetic iron oxide (Fe3O4) nanoparticles from tea waste for arsenic removal. J. Magn. Magn. Mater 356, 21–31.

Luo F, Yang D, Chen Z, Megharaj M, Naidu R, 2016 One-step green synthesis of bimetallic Fe/Pd nanoparticles used to degrade Orange II. J. Hazard. Mater 303, 145–153. [PubMed: 26530891]

Machado S, Stawiński W, Slonina P, Pinto A, Grosso J, Nouws H, Albergaria JT, Delerue-Matos C, 2013 Application of green zero-valent iron nanoparticles to the remediation of soils contaminated with ibuprofen. Sci. Total Environ 461, 323–329. [PubMed: 23738986]

Madhavi V, Prasad T, Reddy AVB, Reddy BR, Madhavi G, 2013 Application of phytogenic zerovalent iron nanoparticles in the adsorption of hexavalent chromium. Spectrochim. Acta A. Mol. Biomol. Spectrosc 116, 17–25. [PubMed: 23896293]

Manjari G, Saran S, Arun T, Rao AVB, Devipriya SP, 2017 Catalytic and recyclability properties of phytogenic copper oxide nanoparticles derived from Aglaia elaeagnoidea flower extract. J. Saudi Chem. Soc. 21, 610–618.

Markova Z, Novak P, Kaslik J, Plachtova P, Brazdova M, Jancula D, Siskova KM, Machala L, Marsalek B, Zboril R, Varma RS, 2014 Iron(II,III)–Polyphenol complex nanoparticles derived from green tea with remarkable ecotoxicological impact. ACS Sustainable Chem. Eng 2, 1674–1680.

Martínez-Cabanas M, López-García M, Barriada JL, Herrero R, Sastre de Vicente ME, 2016 Green synthesis of iron oxide nanoparticles. Development of magnetic hybrid materials for efficient As(V) removal. Chem. Eng. J 301, 83–91.

Martins M, Mourato C, Sanches S, Noronha JP, Crespo MB, Pereira IA, 2017 Biogenic platinum and palladium nanoparticles as new catalysts for the removal of pharmaceutical compounds. Water Res. 108, 160–168. [PubMed: 27817891]

Maruthai J, Muthukumarasamy A, Baskaran B, 2018 Optical, biological and catalytic properties of ZnO/MgO nanocomposites derived via Musa paradisiaca bract extract. Ceram. Int 44, 13152–13160.

Maryami M, Nasrollahzadeh M, Mehdipour E, Sajadi SM, 2016 Preparation of the Ag/RGO nanocomposite by use of Abutilon hirtum leaf extract: a recoverable catalyst for the reduction of organic dyes in aqueous medium at room temperature. Int. J. Hydrogen Energy 41, 21236–21245.

Maryami M, Nasrollahzadeh M, Sajadi SM, 2017 Green synthesis of the Pd/perlite nanocomposite using Euphorbia neriifolia L. Leaf extract and evaluation of its catalytic activity. Sep. Purif. Technol 184, 298–307.

Mehr ES, Sorbiun M, Ramazani A, Fardood ST, 2018 Plant-mediated synthesis of zinc oxide and copper oxide nanoparticles by using ferulago angulata (schlecht) boiss extract and comparison of their photocatalytic degradation of Rhodamine B (RhB) under visible light irradiation. J. Mater. Sci. Mater. Electron 29, 1333–1340.

Miri A, Mousavi SR, Sarani M, Mahmoodi Z, 2018a Using biebersteinia multifida aqueous extract, the photocatalytic activity of synthesized silver nanoparticles. Orient. J. Chem 34, 1513–1517.

Miri A, Vahed HOS, Sarani M, 2018b Biosynthesis of silver nanoparticles and their role in photocatalytic degradation of methylene blue dye. Res. Chem. Intermed 44, 6907–6915.

Mishra A, Kumari M, Pandey S, Chaudhry V, Gupta K, Nautiyal C, 2014 Biocatalytic and antimicrobial activities of gold nanoparticles synthesized by Trichoderma sp. Bioresour. Technol 166, 235–242. [PubMed: 24914997]

Mittal AK, Chisti Y, Banerjee UC, 2013 Synthesis of metallic nanoparticles using plant extracts. Biotechnol. Adv 31, 346–356. [PubMed: 23318667]

Mohamed HH, Alomair NA, Akhtar S, Youssef TE, 2019 Eco-friendly synthesized α-Fe2O3/TiO2 heterojunction with enhanced visible light photocatalytic activity. J. Photochem. Photobiol. A: Chem 382, 111951.

Momeni SS, Nasrollahzadeh M, Rustaiyan A, 2016 Green synthesis of the Cu/ZnO nanoparticles mediated by Euphorbia prolifera leaf extract and investigation of their catalytic activity. J. Colloid Interface Sci. 472, 173–179. [PubMed: 27038280]

Moulton MC, Braydich-Stolle LK, Nadagouda MN, Kunzelman S, Hussain SM, Varma RS, 2010 Synthesis, characterization and biocompatibility of “green” synthesized silver nanoparticles using tea polyphenols. Nanoscale 2, 763–770. [PubMed: 20648322]

Mozia S, Tomaszewska M, Morawski AW, 2007 Photocatalytic membrane reactor (PMR) coupling photocatalysis and membrane distillation—effectiveness of removal of three azo dyes from water. Catal. Today 129, 3–8.

Mukherjee P, Ahmad A, Mandal D, Senapati S, Sainkar SR, Khan MI, Parishcha R, Ajaykumar P, Alam M, Kumar R, 2001 Fungus-mediated synthesis of silver nanoparticles and their immobilization in the mycelial matrix: a novel biological approach to nanoparticle synthesis. Nano Lett. 1, 515–519.

Mukherjee D, Ghosh S, Majumdar S, Annapurna K, 2016 Green synthesis of α-Fe2O3 nanoparticles for arsenic (V) remediation with a novel aspect for sludge management. J. Environ. Chem. Eng 4, 639–650.

Muthukumar H, Matheswaran M, 2015 Amaranthus spinosus leaf extract mediated FeO nanoparticles: physicochemical traits, photocatalytic and antioxidant activity. ACS Sustain. Chem. Eng 3, 3149–3156.

Muthukumar H, Gire A, Kumari M, Manickam M, 2017 Biogenic synthesis of nanobiomaterial for toxic naphthalene photocatalytic degradation optimization and kinetics studies. Int. Biodeterior. Biodegradation 119, 587–594.

Mystrioti C, Xanthopoulou T, Tsakiridis P, Papassiopi N, Xenidis A, 2016 Comparative evaluation of five plant extracts and juices for nanoiron synthesis and application for hexavalent chromium reduction. Sci. Total Environ 539, 105–113. [PubMed: 26356183]

Nadaf NY, Kanase SS, 2016 Biosynthesis of gold nanoparticles by Bacillus marisflavi and its potential in catalytic dye degradation. Arab. J. Chem

Nadagouda MN, Varma RS, 2008 Green synthesis of silver and palladium nanoparticles at room temperature using coffee and tea extract. Green Chem. 10, 859–862.

Nadagouda MN, Castle AB, Murdock RC, Hussain SM, Varma RS, 2010 In vitro biocompatibility of nanoscale zerovalent iron particles (NZVI) synthesized using tea polyphenols. Green Chem. 12, 114–122.

Nair B, Pradeep T, 2002 Coalescence of nanoclusters and formation of submicron crystallites assisted by Lactobacillus strains. Cryst. Growth Des 2, 293–298.

Naraginti S, Sivakumar A, 2014 Eco-friendly synthesis of silver and gold nanoparticles with enhanced bactericidal activity and study of silver catalyzed reduction of 4-nitrophenol. Spectrochim. Acta A. Mol. Biomol. Spectrosc 128, 357–362. [PubMed: 24681320]

Narasaiah P, Mandal BK, Sarada N, 2017 Green synthesis of Pd NPs from Pimpinella tirupatiensis plant extract and their application in photocatalytic activity dye degradation. Materials Science and Engineering Conference Series 022013.

Nasrollahzadeh M, Sajadi SM, Hatamifard A, 2016a Waste chicken eggshell as a natural valuable resource and environmentally benign support for biosynthesis of catalytically active Cu/eggshell, Fe3O4/eggshell and Cu/Fe3O4/eggshell nanocomposites. Appl. Catal. B 191, 209–227.

Nasrollahzadeh M, Atarod M, Sajadi SM, 2016b Green synthesis of the Cu/Fe3O4 nanoparticles using Morinda morindoides leaf aqueous extract: a highly efficient magnetically separable catalyst for the reduction of organic dyes in aqueous medium at room temperature. Appl. Surf. Sci 364, 636–644.

Nasrollahzadeh M, Sajjadi M, Sajadi SM, 2018a Biosynthesis of copper nanoparticles supported on manganese dioxide nanoparticles using Centella asiatica L. Leaf extract for the efficient catalytic reduction of organic dyes and nitroarenes. Chinese J. Catal 39, 109–117.

Nasrollahzadeh M, Issaabadi Z, Sajadi SM, 2018b Green synthesis of Pd/Fe3O4 nanocomposite using Hibiscus tiliaceus L. Extract and its application for reductive catalysis of Cr (VI) and nitro compounds. Sep. Purif. Technol 197, 253–260.

Nasrollahzadeh M, Sajadi SM, Maham M, Kohsari I, 2018c Biosynthesis, characterization and catalytic activity of the Pd/bentonite nanocomposite for base-and ligand-free oxidative hydroxylation of phenylboronic acid and reduction of Chromium (VI) and nitro compounds. Microporous Mesoporous Mater. 271, 128–137.

Nasrollahzadeh M, Sajjadi M, Maham M, Sajadi SM, Barzinjy AA, 2018d Biosynthesis of the palladium/sodium borosilicate nanocomposite using Euphorbia milii extract and evaluation of its catalytic activity in the reduction of chromium (VI), nitro compounds and organic dyes. Mater. Res. Bull 102, 24–35.

Nasrollahzadeh M, Atarod M, Sajjadi M, Sajadi SM, Issaabadi Z, 2019a Plantmediated Green synthesis of nanostructures: mechanisms, characterization, and applications Interface Science and Technology. Elsevier, pp. 199–322.

Nasrollahzadeh M, Sajadi SM, Issaabadi Z, Sajjadi M, 2019b Biological sources used in Green nanotechnology Interface Science and Technology. Elsevier, pp. 81–111.

Nasrollahzadeh M, Mahmoudi-Gom Yek S, Motahharifar N, Ghafori Gorab M, 2019c Recent developments in the plant-mediated green synthesis of Ag-Based nanoparticles for environmental and catalytic applications. Chem. Rec 19, 2436–2479. [PubMed: 31021524]

Nasrollahzadeh M, Sajjadi M, Dadashi J, Ghafuri H, 2020a Pd-based nanoparticles: plant-assisted biosynthesis, characterization, mechanism, stability, catalytic and antimicrobial activities. Adv. Colloid Interface Sci, 102103. [PubMed: 31978638]

Nasrollahzadeh M, Baran T, Baran NY, Sajjadi M, Tahsili MR, Shokouhimehr M, 2020b Pd nanocatalyst stabilized on amine-modified zeolite: antibacterial and catalytic activities for environmental pollution remediation in aqueous medium. Sep. Purif. Technol, 116542.

Nasrollahzadeh M, Akbari R, Issaabadi Z, Sajadi SM, 2020c Biosynthesis and characterization of Ag/MgO nanocomposite and its catalytic performance in the rapid treatment of environmental contaminants. Ceram. Int 46, 2093–2101.

Nasrollahzadeh M, Jaleh B, Baran T, Varma RS, 2020d Efficient degradation of environmental contaminants using Pd-RGO nanocomposite as a retrievable catalyst. Clean Technol. Environ. Policy 22, 325–335.

Nethravathi P, Kumar MP, Suresh D, Lingaraju K, Rajanaika H, Nagabhushana H, Sharma S, 2015 Tinospora cordifolia mediated facile green synthesis of cupric oxide nanoparticles and their photocatalytic, antioxidant and antibacterial properties. Mater. Sci. Semicond. Process 33, 81–88.

Njagi EC, Huang H, Stafford L, Genuino H, Galindo HM, Collins JB, Hoag GE, Suib SL, 2010 Biosynthesis of iron and silver nanoparticles at room temperature using aqueous sorghum bran extracts. Langmuir 27, 264–271. [PubMed: 21133391]

Ojo SA, Lateef A, Azeez MA, Oladejo SM, Akinwale AS, Asafa TB, Yekeen TA, Akinboro A, Oladipo IC, Gueguim-Kana EB, 2016 Biomedical and catalytic applications of gold and silver-gold alloy nanoparticles biosynthesized using cell-free extract ofBacillus SafensisLAU 13: antifungal, dye degradation, anti-coagulant and thrombolytic activities. IEEE Trans. Nanobioscience 15, 433–442. [PubMed: 27164598]

Oremland RS, 1994 Biogeochemical transformations of. Selenium Environ. 389–419.

Paixão RM, Reck IM, Bergamasco R, Vieira MF, Vieira AMS, 2018 Activated carbon of Babassu coconut impregnated with copper nanoparticles by green synthesis for the removal of nitrate in aqueous solution. Environ. Technol 39, 1994–2003. [PubMed: 28639851]

Parandhaman T, Pentela N, Ramalingam B, Samanta D, Das SK, 2016 Metal nanoparticle loaded magnetic-chitosan microsphere: water dispersible and easily separable hybrid metal nano-biomaterial for catalytic applications. ACS Sustain. Chem. Eng 5, 489–501.

Parandhaman T, Dey MD, Das SK, 2019 Biofabrication of supported metal nanoparticles: exploring the bioinspiration strategy to mitigate the environmental challenges. Green Chem. 21, 5469–5500.

Patil SS, Mali MG, Tamboli MS, Patil DR, Kulkarni MV, Yoon H, Kim H, Al-Deyab SS, Yoon SS, Kolekar SS, 2016 Green approach for hierarchical nanostructured Ag-ZnO and their photocatalytic performance under sunlight. Catal. Today 260, 126–134.

Paul B, Bhuyan B, Purkayastha DD, Dhar SS, 2016 Photocatalytic and antibacterial activities of gold and silver nanoparticles synthesized using biomass of Parkia roxburghii leaf. J. Photochem. Photobiol. B, Biol 154, 1–7.

Paul B, Vadivel S, Dhar SS, Debbarma S, Kumaravel M, 2017 One-pot green synthesis of zinc oxide nano rice and its application as sonocatalyst for degradation of organic dye and synthesis of 2-benzimidazole derivatives. J. Phys. Chem. Solids 104, 152–159.

Peng X, Bai X, Cui Z, Liu X, 2019 Green synthesis of Pd truncated octahedrons using of firmiana simplex leaf extract and their catalytic study for electro-oxidation of methanol and reduction of p-nitrophenol. Appl. Organomet. Chem e5045.

Philipse AP, Maas D, 2002 Magnetic colloids from magnetotactic bacteria: chain formation and colloidal stability. Langmuir 18, 9977–9984.

Plachtová P, Medříková Z, Zbořil R, Tuček J, Varma RS, Maršálek B, 2018 Iron and Iron oxide nanoparticles synthesized using green tea extract: improved ecotoxicological profile and ability to degrade malachite green. ACS Sustain. Chem. Eng. 6, 8679–8687.

Poguberović SS, Krčmar DM, Maletić SP, Kónya Z, Pilipović DDT, Kerkez DV, Rončević SD, 2016 Removal of As (III) and Cr (VI) from aqueous solutions using “green” zero-valent iron nanoparticles produced by oak, mulberry and cherry leaf extracts. Ecol. Eng 90, 42–49.

Pradhan N, Pal A, Pal T, 2001 Catalytic reduction of aromatic nitro compounds by coinage metal nanoparticles. Langmuir 17, 1800–1802.

Prasad KS, Gandhi P, Selvaraj K, 2014 Synthesis of green nano iron particles (GnIP) and their application in adsorptive removal of As (III) and As (V) from aqueous solution. Appl. Surf. Sci 317, 1052–1059.

Prasad AR, Garvasis J, Oruvil SK, Joseph A, 2019 Bio-inspired green synthesis of zinc oxide nanoparticles using Abelmoschus esculentus mucilage and selective degradation of cationic dye pollutants. J. Phys. Chem. Solids 127, 265–274.

Qu Y, Pei X, Shen W, Zhang X, Wang J, Zhang Z, Li S, You S, Ma F, Zhou J, 2017 Biosynthesis of gold nanoparticles by Aspergillum sp. WL-Au for degradation of aromatic pollutants. Physica E Low. Syst. Nanostruct 88, 133–141.

Raj R, Dalei K, Chakraborty J, Das S, 2016 Extracellular polymeric substances of a marine bacterium mediated synthesis of CdS nanoparticles for removal of cadmium from aqueous solution. J. Colloid Interface Sci. 462, 166–175. [PubMed: 26454375]

Rajendaran K, Muthuramalingam R, Ayyadurai S, 2019 Green synthesis of Ag-Mo/CuO nanoparticles using Azadirachta indica leaf extracts to study its solar photocatalytic and antimicrobial activities. Mater. Sci. Semicond. Process 91, 230–238.

Ramesh A, Devi DR, Battu G, Basavaiah K, 2018 A Facile plant mediated synthesis of silver nanoparticles using an aqueous leaf extract of Ficus hispida Linn. F. For catalytic, antioxidant and antibacterial applications. South Afr. J. Chem. Eng 26, 25–34.

Ranjith R, Renganathan V, Chen S-M, Selvan NS, Rajam PS, 2019 Green synthesis of reduced graphene oxide supported TiO2/Co3O4 nanocomposite for photocatalytic degradation of methylene blue and crystal violet. Ceram. Int 45, 12926–12933.

Rao A, Bankar A, Kumar AR, Gosavi S, Zinjarde S, 2013 Removal of hexavalent chromium ions by Yarrowia lipolytica cells modified with phyto-inspired Fe0/Fe3O4 nanoparticles. J. Contam. Hydrol 146, 63–73. [PubMed: 23422514]

Ravikumar KVG, Kubendiran H, Ramesh K, Rani S, Mandal TK, Pulimi M, Natarajan C, Mukherjee A, 2020 Batch and column study on tetracycline removal using green synthesized NiFe nanoparticles immobilized alginate beads. Environ. Technol. Innov 17, 100520.

Renuka L, Anantharaju K, Sharma S, Nagaswarupa H, Prashantha S, Nagabhushana H, Vidya Y, 2016 Hollow microspheres Mg-doped ZrO2 nanoparticles: green assisted synthesis and applications in photocatalysis and photoluminescence. J. Alloys. Compd 672, 609–622.

Rizzo L, Meric S, Guida M, Kassinos D, Belgiorno V, 2009 Heterogenous photocatalytic degradation kinetics and detoxification of an urban wastewater treatment plant effluent contaminated with pharmaceuticals. Water Res. 43, 4070–4078. [PubMed: 19596131]

Robati D, Mirza B, Rajabi M, Moradi O, Tyagi I, Agarwal S, Gupta V, 2016 Removal of hazardous dyes-BR 12 and methyl orange using graphene oxide as an adsorbent from aqueous phase. Chem. Eng. J 284, 687–697.

Rosbero TMS, Camacho DH, 2017 Green preparation and characterization of tentacle-like silver/copper nanoparticles for catalytic degradation of toxic chlorpyrifos in water. J. Environ. Chem. Eng 5, 2524–2532.

Rouch DA, Lee BT, Morby AP, 1995 Understanding cellular responses to toxic agents: a model for mechanism-choice in bacterial metal resistance. J. Ind. Microbiol 14, 132–141. [PubMed: 7766205]

Saad M, Tahir H, Ali D, 2017 Green synthesis of Ag-Cr-AC nanocomposites by Azadirachta indica and its application for the simultaneous removal of binary mixture of dyes by ultrasonicated assisted adsorption process using Response Surface Methodology. Ultrason. Sonochem 38, 197–213. [PubMed: 28633820]

Sajadi SM, Kolo K, Hamad SM, Mahmud SA, Barzinjy AA, Hussein SM, 2018 Green synthesis of the Ag/Bentonite nanocomposite UsingEuphorbia larica extract: a reusable catalyst for efficient reduction of nitro compounds and organic dyes. ChemistrySelect 3, 12274–12280.

Sarkar A, Jana S, 1986 Heavy metal pollutant tolerance of Azolla pinnata. Water Air Soil Pollut. 27, 15–18.

Sastry M, Ahmad A, Khan MI, Kumar R, 2003 Biosynthesis of metal nanoparticles using fungi and actinomycete. Curr. Sci 85, 162–170.

Sengani M, Grumezescu AM, Rajeswari VD, 2017 Recent trends and methodologies in gold nanoparticle synthesis–A prospective review on drug delivery aspect. OpenNano 2, 37–46.

Sharma S, 2016 ZnO nano-flowers from Carica papaya milk: degradation of Alizarin Red-S dye and antibacterial activity against Pseudomonas aeruginosa and Staphylococcus aureus. Optik 127, 6498–6512.

Sharmila G, Thirumarimurugan M, Sivakumar VM, 2016 Optical, catalytic and antibacterial properties of phytofabricated CuO nanoparticles using Tecoma castanifolia leaf extract. Optik 127, 7822–7828.

Shen W, Qu Y, Pei X, Li S, You S, Wang J, Zhang Z, Zhou J, 2017 Catalytic reduction of 4-nitrophenol using gold nanoparticles biosynthesized by cell-free extracts of Aspergillus sp. WL-Au, J. hazardous mater 321, 299–306.

Shivaji K, Monica ES, Devadoss A, Kirubakaran DD, Dhas CR, Jain SM, 2020 Synthesizing Green photocatalyst using plant leaf extract for Water pollutant treatment In: Pitchaimuthu S, Naushad M, Rajendran S, Lichtfouse E (Eds.), Green Photocatalysts. Environmental Chemistry for a Sustainable World, Springer, Cham.

Shukla AK, Iravani S, 2017 Metallic nanoparticles: green synthesis and spectroscopic characterization. Environ. Chem. Lett 15, 223–231.

Singh P, Kim Y-J, Zhang D, Yang D-C, 2016 Biological synthesis of nanoparticles from plants and microorganisms. Trends Biotechnol. 34, 588–599. [PubMed: 26944794]

Singh S, Kumar N, Kumar M, Agarwal A, Mizaikoff B, 2017 Electrochemical sensing and remediation of 4-nitrophenol using bio-synthesized copper oxide nanoparticles. Chem. Eng. J 313, 283–292.

Sinha T, Ahmaruzzaman M, 2015 Biogenic synthesis of Cu nanoparticles and its degradation behavior for methyl red. Mater. Lett 159, 168–171.

Sinha AK, Basu M, Sarkar S, Pradhan M, Pal T, 2013 Synthesis of gold nanochains via photoactivation technique and their catalytic applications. J. Colloid Interface Sci 398, 13–21. [PubMed: 23473571]

Sinha T, Ahmaruzzaman M, Adhikari PP, Bora R, 2017 Green and environmentally sustainable fabrication of Ag-SnO2 nanocomposite and its multifunctional efficacy as photocatalyst and antibacterial and antioxidant agent. ACS Sustain. Chem. Eng 5, 4645–4655.

Slawson RM, Van Dyke MI, Lee H, Trevors JT, 1992 Germanium and silver resistance, accumulation, and toxicity in microorganisms. Plasmid 27, 72–79. [PubMed: 1741462]

Smuleac V, Varma R, Sikdar S, Bhattacharyya D, 2011 Green synthesis of Fe and Fe/Pd bimetallic nanoparticles in membranes for reductive degradation of chlorinated organics. J. Memb. Sci 379, 131–137. [PubMed: 22228920]

Sohrabnezhad S, Seifi A, 2016 The green synthesis of Ag/ZnO in montmorillonite with enhanced photocatalytic activity. Appl. Surf. Sci 386, 33–40.

Solano RA, Herrera AP, Maestre D, Cremades A, 2019 Fe-TiO2 nanoparticles synthesized by green chemistry for potential application in waste water photocatalytic treatment. J. Nanotechnol 2019, 1–11.

Sood A, Uniyal PL, Prasanna R, Ahluwalia AS, 2012 Phytoremediation potential of aquatic macrophyte, Azolla. Ambio 41, 122–137. [PubMed: 22396093]

Sreeju N, Rufus A, Philip D, 2017 Studies on catalytic degradation of organic pollutants and anti-bacterial property using biosynthesized CuO nanostructures. J. Mol. Liq 242, 690–700.

Srivastava N, Mukhopadhyay M, 2014 Biosynthesis of SnO2 nanoparticles using bacterium Erwinia herbicola and their photocatalytic activity for degradation of dyes. Ind. Eng. Chem. Res 53, 13971–13979.

Srivastava V, Sharma Y, Sillanpää M, 2015 Green synthesis of magnesium oxide nanoflower and its application for the removal of divalent metallic species from synthetic wastewater. Ceram. Int 41, 6702–6709.

Stan M, Lung I, Soran M-L, Leostean C, Popa A, Stefan M, Lazar MD, Opris O, Silipas T-D, Porav AS, 2017 Removal of antibiotics from aqueous solutions by green synthesized magnetite nanoparticles with selected agro-waste extracts. Process. Saf. Environ. Prot 107, 357–372.

Stephen JR, Macnaughtont SJ, 1999 Developments in terrestrial bacterial remediation of metals. Curr. Opin. Biotechnol 10, 230–233. [PubMed: 10361068]

Suárez-Cerda J, Alonso-Nuñez G, Espinoza-Gómez H, Flores-López LZ, 2015 Synthesis, kinetics and photocatalytic study of “ultra-small” Ag-NPs obtained by a green chemistry method using an extract of Rosa ‘andeli’double delight petals. J. Colloid Interface Sci 458, 169–177. [PubMed: 26218196]

Sudhaparimala S, Vaishnavi M, 2016 Biological synthesis of nano composite SnO2-ZnO–screening for efficient photocatalytic degradation and antimicrobial activity. Mater. Today Proc 3, 2373–2380.

Sureshkumar M, Siswanto DY, Lee C-K, 2010 Magnetic antimicrobial nanocomposite based on bacterial cellulose and silver nanoparticles. J. Mater. Chem 20, 6948–6955.

Sweeney RY, Mao C, Gao X, Burt JL, Belcher AM, Georgiou G, Iverson BL, 2004 Bacterial biosynthesis of cadmium sulfide nanocrystals. Chem. Biol 11, 1553–1559. [PubMed: 15556006]

Tajbakhsh M, Alinezhad H, Nasrollahzadeh M, Kamali TA, 2016 Green synthesis of the Ag/HZSM-5 nanocomposite by using Euphorbia heterophylla leaf extract: a recoverable catalyst for reduction of organic dyes. J. Alloys. Compd 685, 258–265.

Tamuly C, Hazarika M, Bordoloi M, Bhattacharyya PK, Kar R, 2014 Biosynthesis of Ag nanoparticles using pedicellamide and its photocatalytic activity: an ecofriendly approach. Spectrochim. Acta A. Mol. Biomol. Spectrosc 132, 687–691. [PubMed: 24907972]

Thapa R, Bhagat C, Shrestha P, Awal S, Dudhagara P, 2017 Enzyme-mediated formulation of stable elliptical silver nanoparticles tested against clinical pathogens and MDR bacteria and development of antimicrobial surgical thread. Ann. Clin. Microbiol. Antimicrob 16, 39. [PubMed: 28511708]

Toyao T, Saito M, Horiuchi Y, Mochizuki K, Iwata M, Higashimura H, Matsuoka M, 2013 Efficient hydrogen production and photocatalytic reduction of nitrobenzene over a visible-light-responsive metal–organic framework photocatalyst. Catal. Sci. Technol 3, 2092–2097.

Tu J, Yang Z, Hu C, 2015 Efficient catalytic aerobic oxidation of chlorinated phenols with mixed-valent manganese oxide nanoparticles. J. Chem. Technol. Biotechnol 90, 80–86.

Turunc E, Binzet R, Gumus I, Binzet G, Arslan H, 2017 Green synthesis of silver and palladium nanoparticles using Lithodora hispidula (Sm.) Griseb.(Boraginaceae) and application to the electrocatalytic reduction of hydrogen peroxide. Mater. Chem. Phys 202, 310–319.

Tyagi S, Rawtani D, Khatri N, Tharmavaram M, 2018 Strategies for nitrate removal from aqueous environment using nanotechnology: a review. J. Water Process. Eng 21, 84–95.

Ullah H, Wilfred CD, Shaharun MS, 2017 Synthesis of silver nanoparticles using ionic-liquid-Based microwave-assisted extraction from Polygonum minus and photodegradation of methylene blue. J. Chinese Chem. Soc 64, 1164–1171.

Vanaamudan A, Soni H, Sudhakar PP, 2016 Palm shell extract capped silver nanoparticles-as efficient catalysts for degradation of dyes and as SERS substrates. J. Mol. Liq 215, 787–794.

Varadavenkatesan T, Lyubchik E, Pai S, Pugazhendhi A, Vinayagam R, Selvaraj R, 2019 Photocatalytic degradation of Rhodamine B by zinc oxide nanoparticles synthesized using the leaf extract of Cyanometra ramiflora. J. Photochem. Photobiol. B, Biol 199, 111621.

Vellaichamy B, Periakaruppan P, 2016a A facile, one-pot and eco-friendly synthesis of gold/silver nanobimetallics smartened rGO for enhanced catalytic reduction of hexavalent chromium. RSC Adv. 6, 57380–57388.

Vellaichamy B, Periakaruppan P, 2016b Silver nanoparticle-embedded RGO-nanosponge for superior catalytic activity towards 4-nitrophenol reduction. RSC Adv. 6, 88837–88845.

Vennila M, Prabha N, 2015 Plant mediated green synthesis of silver nano particles from the plant extract of Morinda tinctoria and its application in effluent water treatment. Int. J. Chemtech Res 7, 2993–2999.

Vidya C, Manjunatha C, Chandraprabha M, Rajshekar M, Mal AR, 2017 Hazard free green synthesis of ZnO nano-photo-catalyst using Artocarpus heterophyllus leaf extract for the degradation of Congo red dye in water treatment applications. J. Environ. Chem. Eng 5, 3172–3180.

Vijayan R, Joseph S, Mathew B, 2018 Eco-friendly synthesis of silver and gold nanoparticles with enhanced antimicrobial, antioxidant, and catalytic activities. IET Nanobiotechnol. 12, 850–856. [PubMed: 30104462]

Wang Y-T, 2000 Microbial reduction of chromate, in: environmental microbe-metal interactions. Abstr. Gen. Meet. Am. Soc. Microbiol 225–235.

Wang Z, 2013 Iron complex nanoparticles synthesized by eucalyptus leaves. ACS Sustain. Chem. Eng 1, 1551–1554.

Wang T, Jin X, Chen Z, Megharaj M, Naidu R, 2014a Green synthesis of Fe nanoparticles using eucalyptus leaf extracts for treatment of eutrophic wastewater. Sci. Total Environ 466, 210–213. [PubMed: 23895784]

Wang Z, Fang C, Megharaj M, 2014b Characterization of iron–polyphenol nanoparticles synthesized by three plant extracts and their fenton oxidation of azo dye. ACS Sustain. Chem. Eng 2, 1022–1025.

Wang T, Lin J, Chen Z, Megharaj M, Naidu R, 2014c Green synthesized iron nanoparticles by green tea and eucalyptus leaves extracts used for removal of nitrate in aqueous solution. J. Clean. Prod 83, 413–419.

Wang Z, Xu C, Li X, Liu Z, 2015 In situ green synthesis of Ag nanoparticles on tea polyphenols-modified graphene and their catalytic reduction activity of 4-nitrophenol. Colloids Surf. A Physicochem. Eng. Asp 485, 102–110.

Wang H, Yuan X, Wang H, Chen X, Wu Z, Jiang L, Xiong W, Zeng G, 2016 Facile synthesis of Sb2S3/ultrathin g-C_3N_4 sheets heterostructures embedded with g-C_3N_4 quantum dots with enhanced NIR-light photocatalytic performance. Appl. Catal. B 193, 36–46.

Wang R, Wang S, Tai Y, Tao R, Dai Y, Guo J, Yang Y, Duan S, 2017 Biogenic manganese oxides generated by green algae Desmodesmus sp. WR1 to improve bisphenol A removal. J. Hazard. Mater 339, 310–319. [PubMed: 28658640]

Wang X, Zhang D, Qian H, Liang Y, Pan X, Gadd GM, 2018 Interactions between biogenic selenium nanoparticles and goethite colloids and consequence for remediation of elemental mercury contaminated groundwater. Sci. Total Environ 613, 672–678. [PubMed: 28938209]

Wei Y, Fang Z, Zheng L, Tsang EP, 2017 Biosynthesized iron nanoparticles in aqueous extracts of Eichhornia crassipes and its mechanism in the hexavalent chromium removal. Appl. Surf. Sci 399, 322–329.

Weng X, Huang L, Chen Z, Megharaj M, Naidu R, 2013 Synthesis of iron-based nanoparticles by green tea extract and their degradation of malachite. Ind. Crops Prod 51, 342–347.

Weng X, Jin X, Lin J, Naidu R, Chen Z, 2016 Removal of mixed contaminants Cr (VI) and Cu (II) by green synthesized iron based nanoparticles. Ecol. Eng 97, 32–39.

Wu Z, Su X, Lin Z, Owens G, Chen Z, 2019 Mechanism of As(V) removal by green synthesized iron nanoparticles. J. Hazard. Mater 379, 120811. [PubMed: 31254786]

Xiao Z, Yuan M, Yang B, Liu Z, Huang J, Sun D, 2016 Plant-mediated synthesis of highly active iron nanoparticles for Cr (VI) removal: investigation of the leading biomolecules. Chemosphere 150, 357–364. [PubMed: 26921588]

Xu C, Nasrollahzadeh M, Sajjadi M, Maham M, Luque R, Puente-Santiago AR, 2019 Benign-by-design nature-inspired nanosystems in biofuels production and catalytic applications. Renew. Sustain. Energy Rev 112, 195–252.

Xu Q, Li W, Ma L, Cao D, Owens G, Chen Z, 2020 Simultaneous removal of ammonia and phosphate using green synthesized iron oxide nanoparticles dispersed onto zeolite. Sci. Total Environ 703, 135002. [PubMed: 31726293]

Yadav IC, Devi NL, Syed JH, Cheng Z, Li J, Zhang G, Jones KC, 2015 Current status of persistent organic pesticides residues in air, water, and soil, and their possible effect on neighboring countries: a comprehensive review of India. Sci. Total Environ 511, 123–137. [PubMed: 25540847]

Yaqoob AA, Parveen T, Umar K, Mohamad Ibrahim MN, 2020 Role of nanomaterials in the treatment of wastewater: a review. Water 12, 495.

Yi H, Jiang M, Huang D, Zeng G, Lai C, Qin L, Zhou C, Li B, Liu X, Cheng M, 2018 Advanced photocatalytic Fenton-like process over biomimetic hemin-Bi2WO6 with enhanced pH. J. Taiwan Inst. Chem. Eng 93, 184–192.

Yi H, Yan M, Huang D, Zeng G, Lai C, Li M, Huo X, Qin L, Liu S, Liu X, 2019 Synergistic effect of artificial enzyme and 2D nano-structured Bi2WO6 for ecofriendly and efficient biomimetic photocatalysis. Appl. Catal. B 250, 52–62.

Yu ZT, Liao ZL, Jiang YS, Li GH, Chen JS, 2005 Water-insoluble Ag–U–Organic assemblies with photocatalytic activity. Chem. Eur. J 11, 2642–2650. [PubMed: 15729678]

Zare M, Namratha K, Thakur M, Byrappa K, 2019 Biocompatibility assessment and photocatalytic activity of bio-hydrothermal synthesis of ZnO nanoparticles by Thymus vulgaris leaf extract. Mater. Res. Bull 109, 49–59.

Zhang C, Liu S, Logan J, Mazumder R, Phelps TJ, 1996 Enhancement of Fe (III), Co (III), and Cr (VI) reduction at elevated temperatures and by a thermophilic bacterium. Appl. Biochem. Biotechnol 57, 923–932.

Zhang C, Vali H, Romanek CS, Phelps TJ, Liu SV, 1998 Formation of singledomain magnetite by a thermophilic bacterium. Am. Mineral 83, 1409–1418.

Zhang X, Lin M, Lin X, Zhang C, Wei H, Zhang H, Yang B, 2014 Polypyrroleenveloped Pd and Fe3O4 nanoparticle binary hollow and bowl-like superstructures as recyclable catalysts for industrial wastewater treatment. ACS Appl. Mater. Interfaces 6, 450–458. [PubMed: 24266702]

Zhang P, Hou D, O'Connor D, Li X, Pehkonen S, Varma RS, Wang X, 2018 Green and size-specific synthesis of stable Fe–Cu oxides as earth-abundant adsorbents for malachite green removal. ACS Sustain. Chem. Eng 6, 9229–9236.

Zhang W, Zhang D, Liang Y, 2019 Nanotechnology in remediation of water contaminated by poly- and perfluoroalkyl substances: a review. Environ. Pollut 247, 266–276. [PubMed: 30685667]

Zheng Y, Wang Z, Peng F, Fu L, 2017 Biosynthesis of silver nanoparticles by Plectranthus amboinicus leaf extract and their catalytic activity towards methylene blue degradation. Revista Mexicana de Ingeniería Química 16, 41–45.

Zhou D, Kim D-G, Ko S-O, 2015 Heavy metal adsorption with biogenic manganese oxides generated by Pseudomonas putida strain MnB1. J. Ind. Eng. Chem 24, 132–139.

Zhuang Z, Huang L, Wang F, Chen Z, 2015 Effects of cyclodextrin on the morphology and reactivity of iron-based nanoparticles using Eucalyptus leaf extract. Ind. Crops Prod 69, 308–313.

Zinatloo-Ajabshir S, Salehi Z, Salavati-Niasari M, 2018a Green synthesis and characterization of Dy2Ce2O7 ceramic nanostructures with good photocatalytic properties under visible light for removal of organic dyes in water. J. Clean. Prod 192, 678–687.

Zinatloo-Ajabshir S, Morassaei MS, Salavati-Niasari M, 2018b Nd2Sn2O7 nanostructures as highly efficient visible light photocatalyst: green synthesis using pomegranate juice and characterization. J. Clean. Prod 198, 11–18.

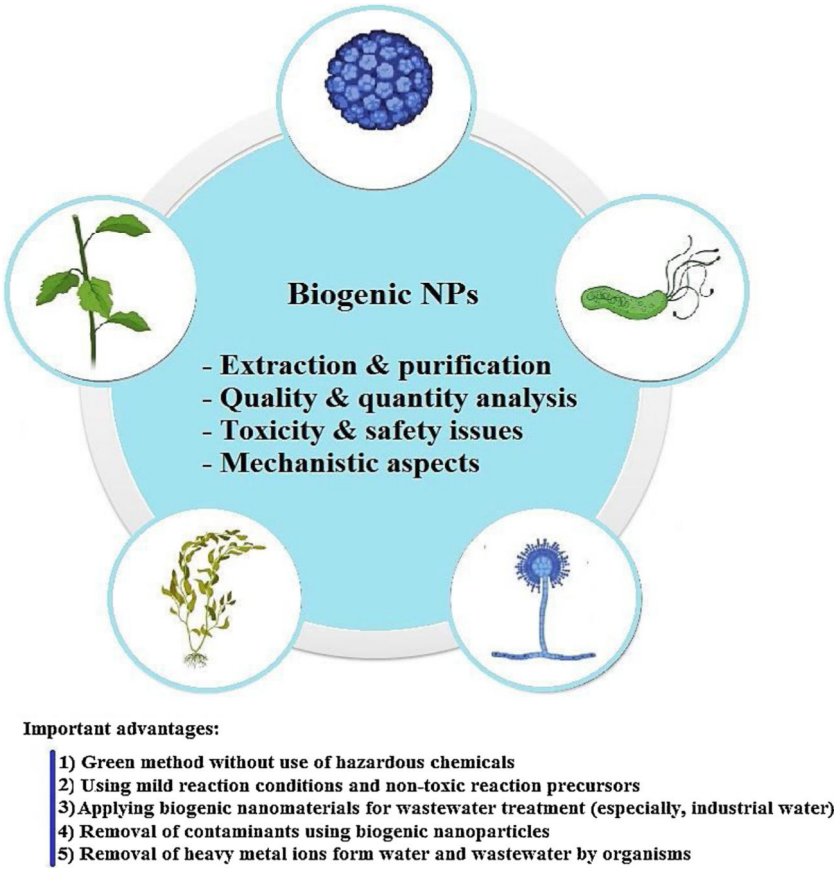

Fig. 1.

Biogenic nanomaterials for wastewater treatment: notable advantages and challenges.

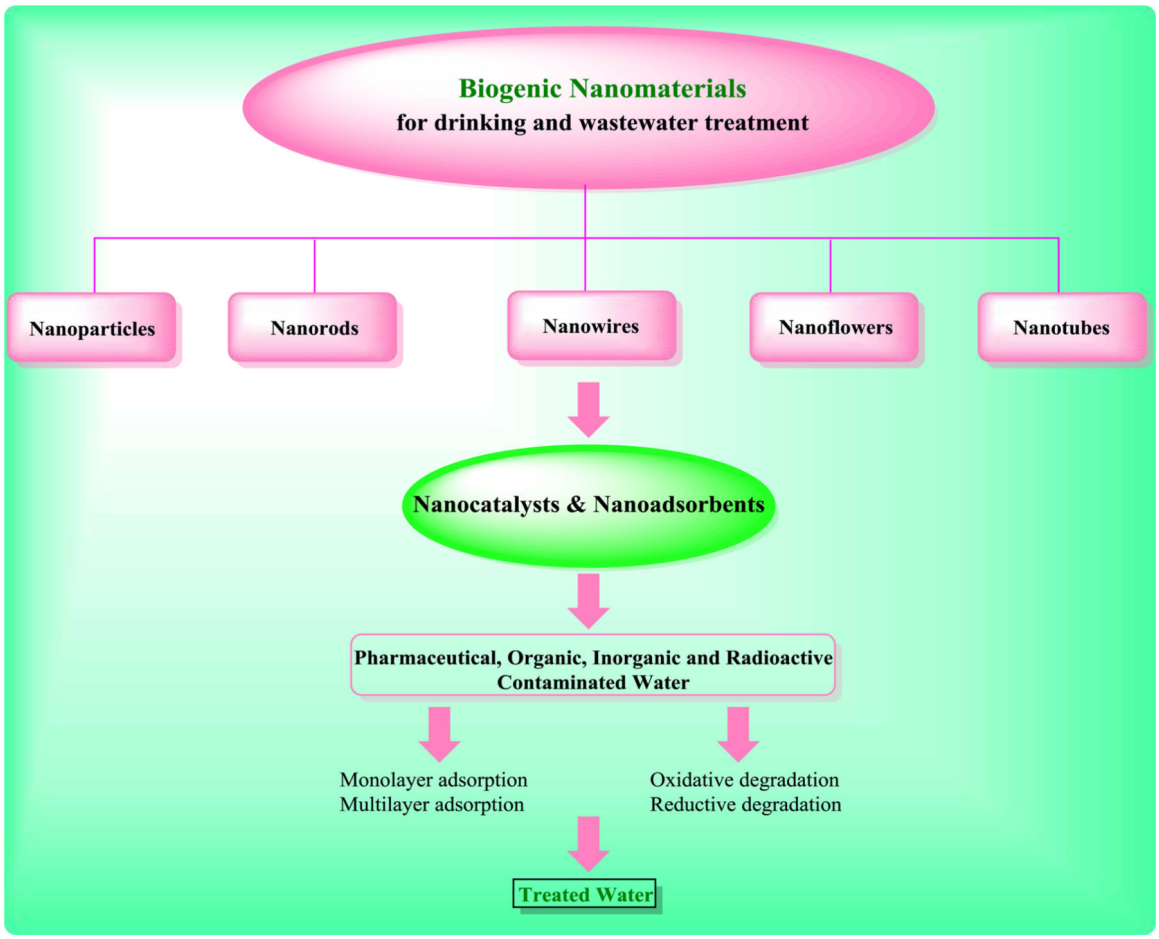

Fig. 2.
Categories of biogenic nanomaterials for appliances in wastewater treatment.

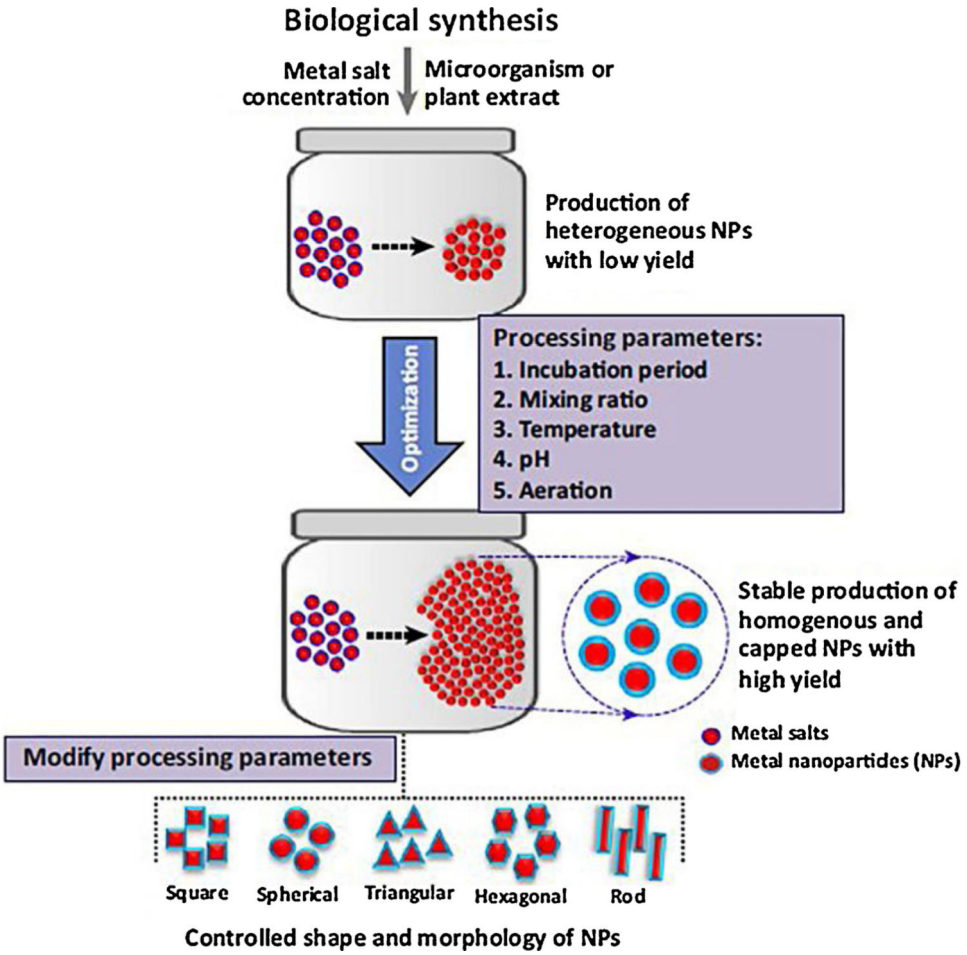

Fig. 3.

Parameters for the fabrication of monodispersed and stable NPs. Reproduced with permission from Ref (Singh et al., 2016).

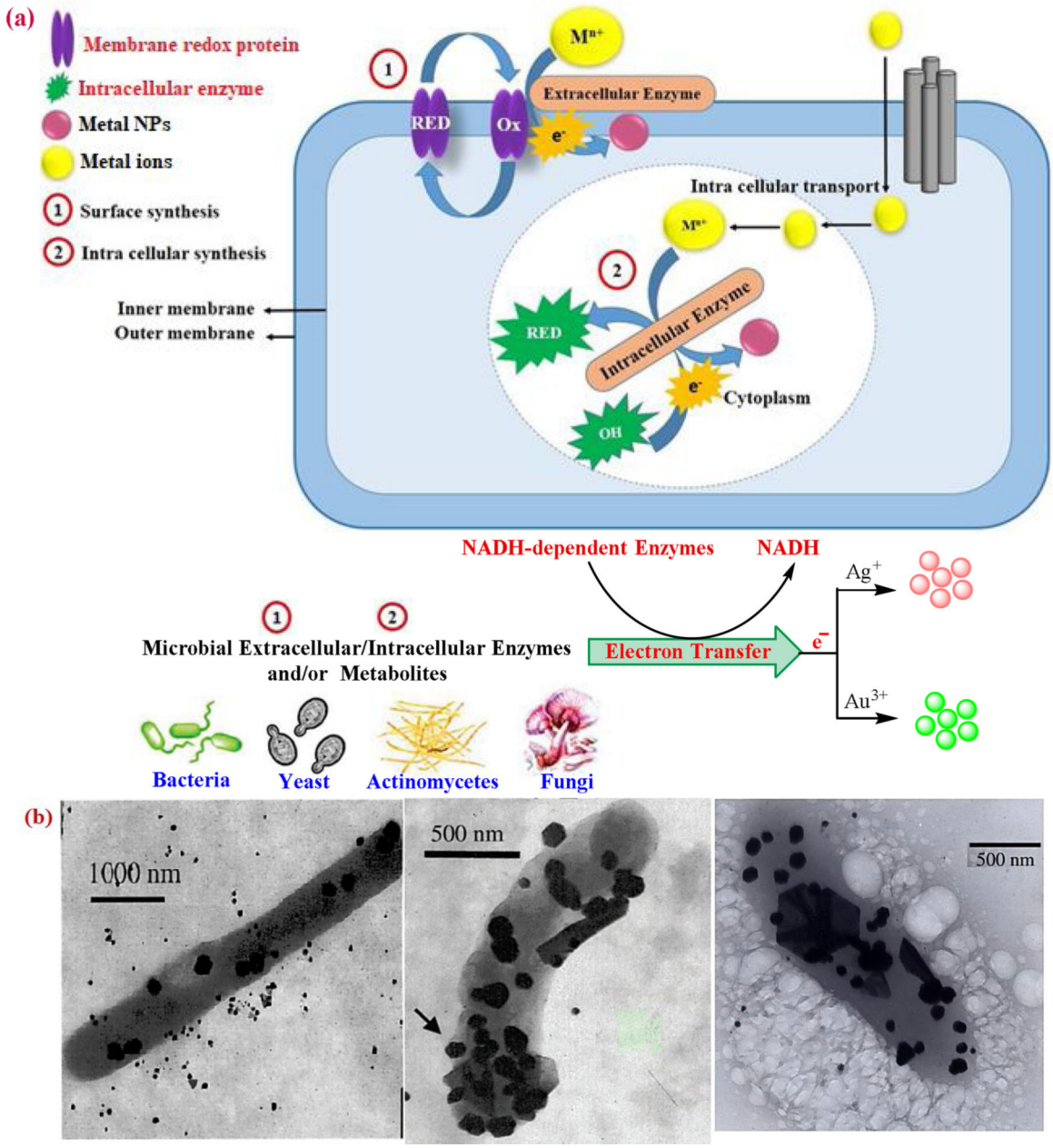

Fig. 4.

(a) Mechanism of extracellular/intracellular synthesis of NPs by microbial enzymes and/or metabolites. (b) *Lactobacillus* bacterial cell can serve as support and reducing agent for the formation of NPs. Reprinted with permission from Refs (Sengani et al., 2017; Parandhaman et al., 2019; Nair and Pradeep, 2002).

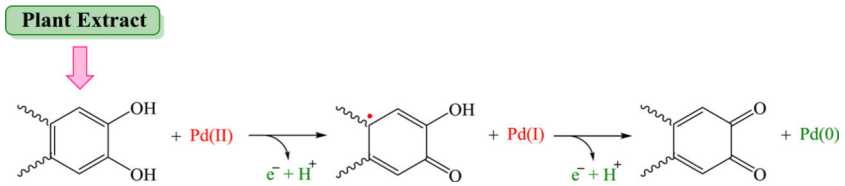

Fig. 5.

Proposed reaction mechanism for the green-synthesized Pd nanomaterials. Redrawn from Ref (Nasrollahzadeh et al., 2020a).

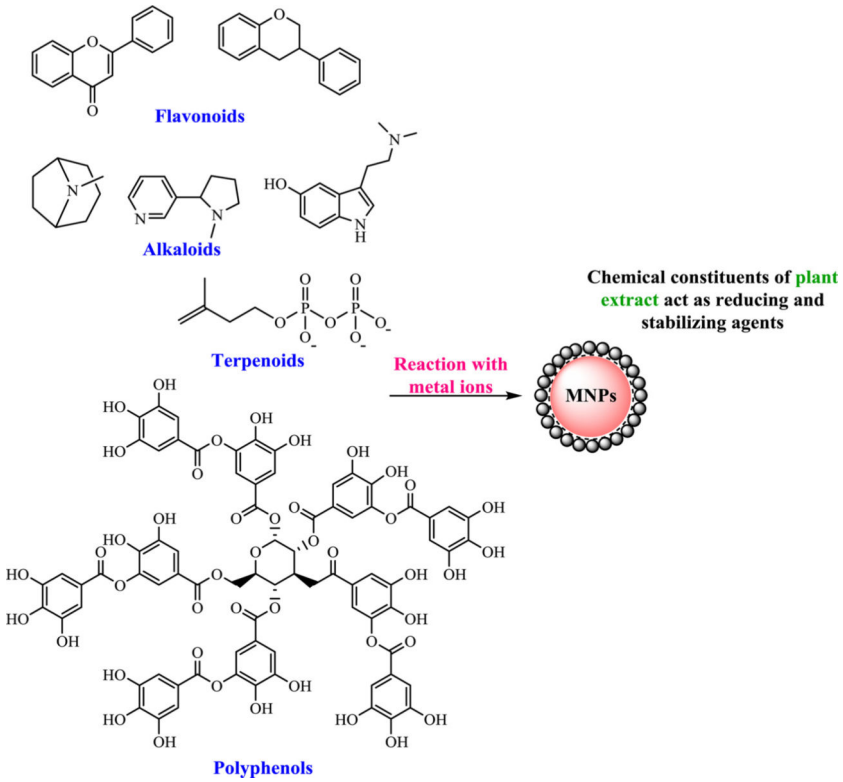

Fig. 6.

Probable components of various plant extracts towards the reduction of metal ions to metal NPs. Redrawn from Ref (Mittal et al., 2013).

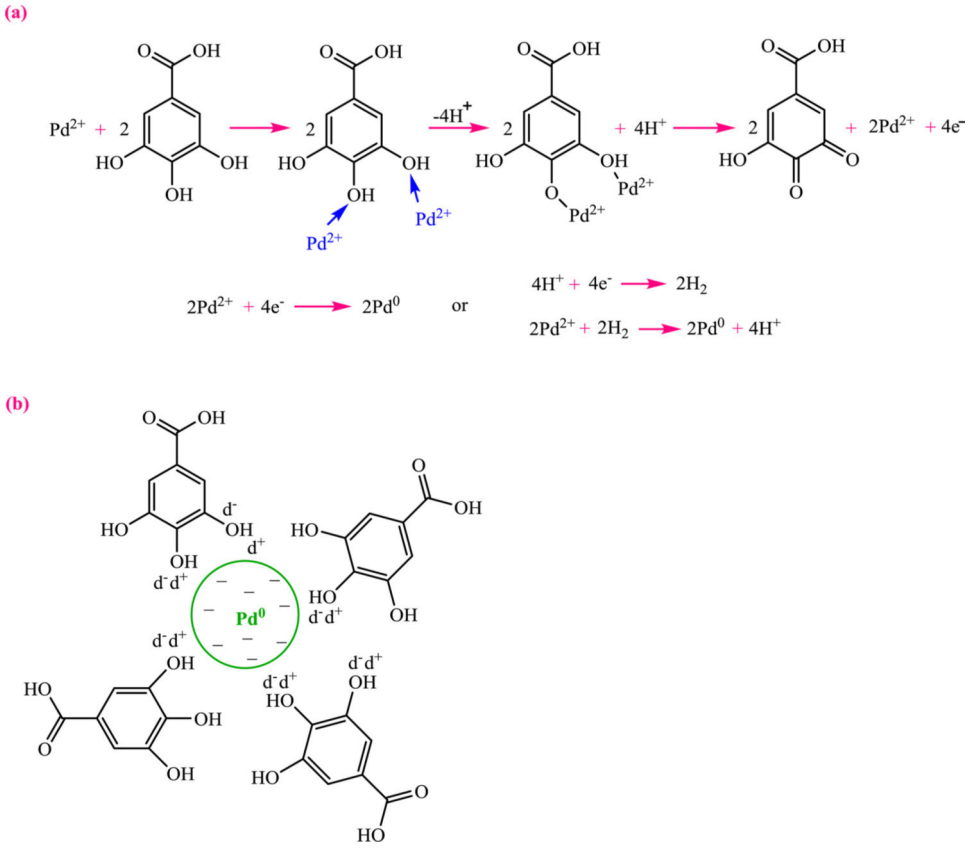

Fig. 7.

Gallic acid-assisted (a) Pd(II) reduction and (b) Pd NPs stabilization. Redrawn from Ref (Dauthal and Mukhopadhyay, 2013).

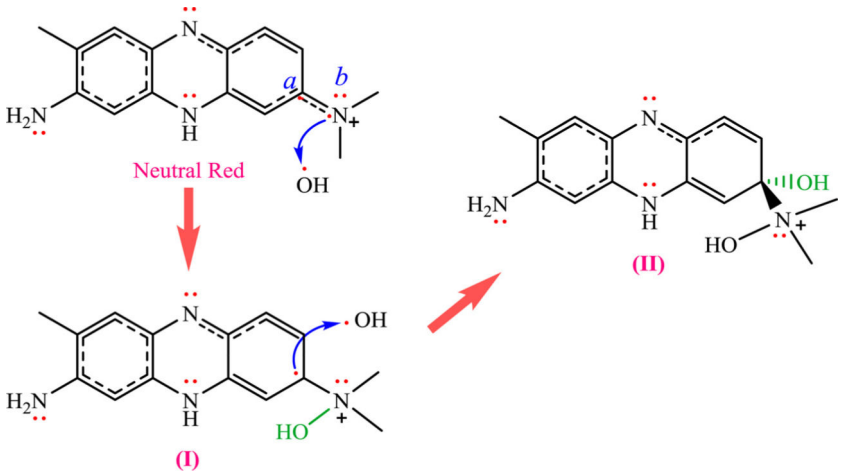

Fig. 8.

Initial step proposed for the reaction of NR dye with hydroxyl radical. Redrawn from Ref (Jaafar et al., 2019).

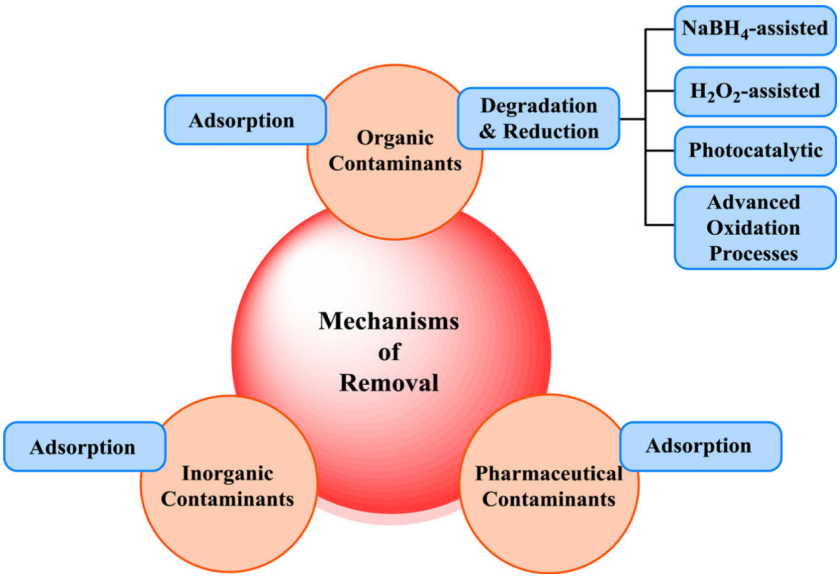

Fig. 9.

Removal of pollutants by applying nanomaterials. Redrawn from Ref (Eskandarloo et al., 2017).

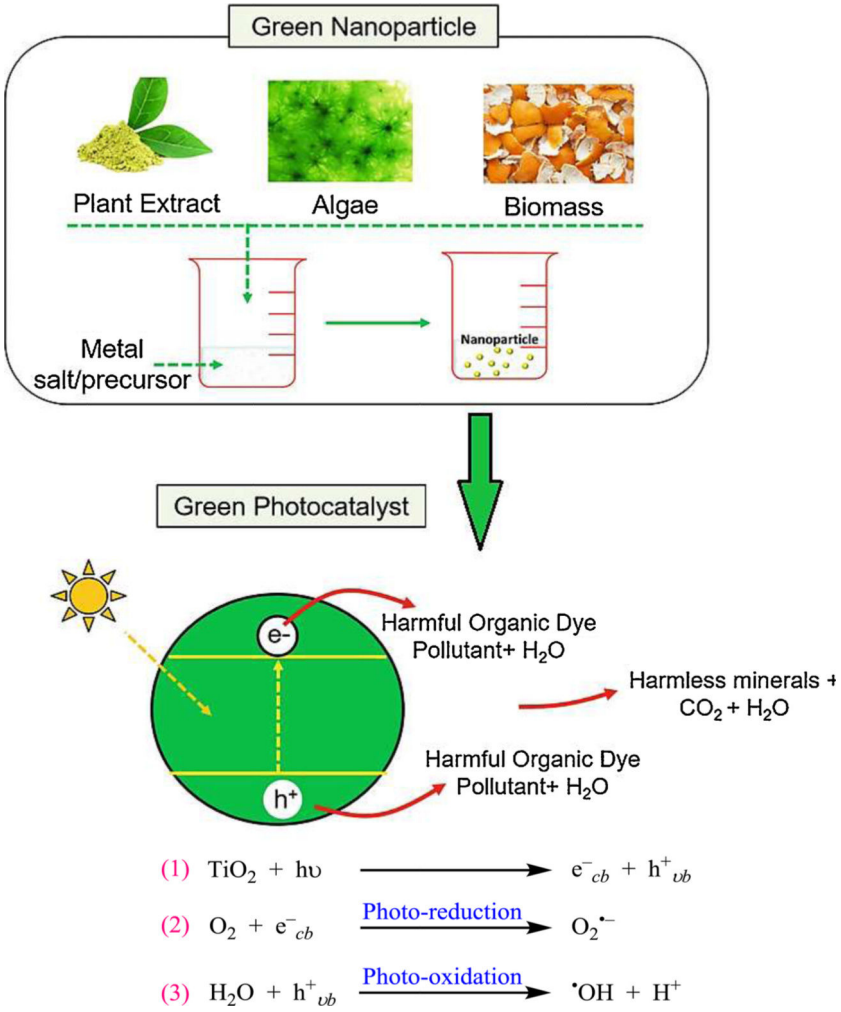

Fig. 10.

Schematic representation and general mechanism for photocatalytic degradation of dye using green-synthesized NPs. Reproduced with permission from Ref (Shivaji et al., 2020).

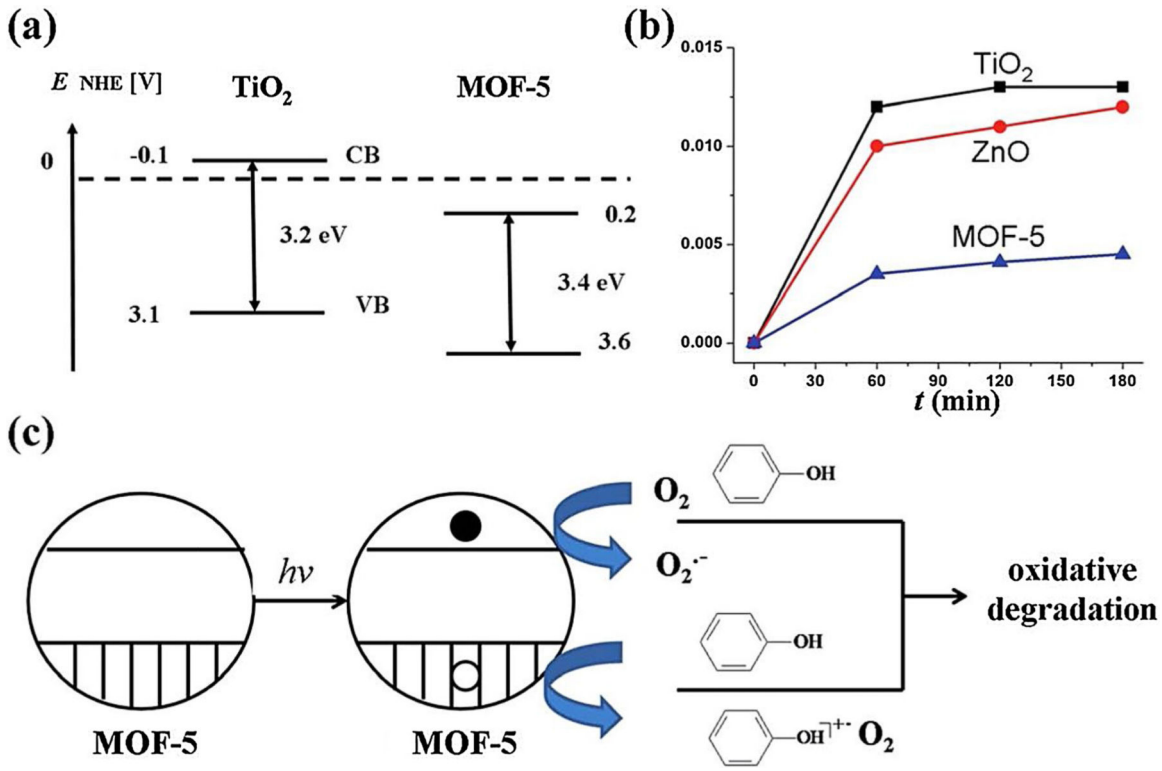

Fig. 11.

(a) Calculated values of the band gaps and position of the conduction and valence bands (CB and VB) for MOF-5 in comparison with those of commercial TiO_2. (b) A time conversion plot of the phenol disappearance (*y* axis represents "mol of phenol decomposed per g per mol"). (c) A possible mechanistic proposal towards the photodegradation of phenol utilizing MOF-5 photocatalyst. Reproduced with permission from Ref (Alvaro et al., 2007).

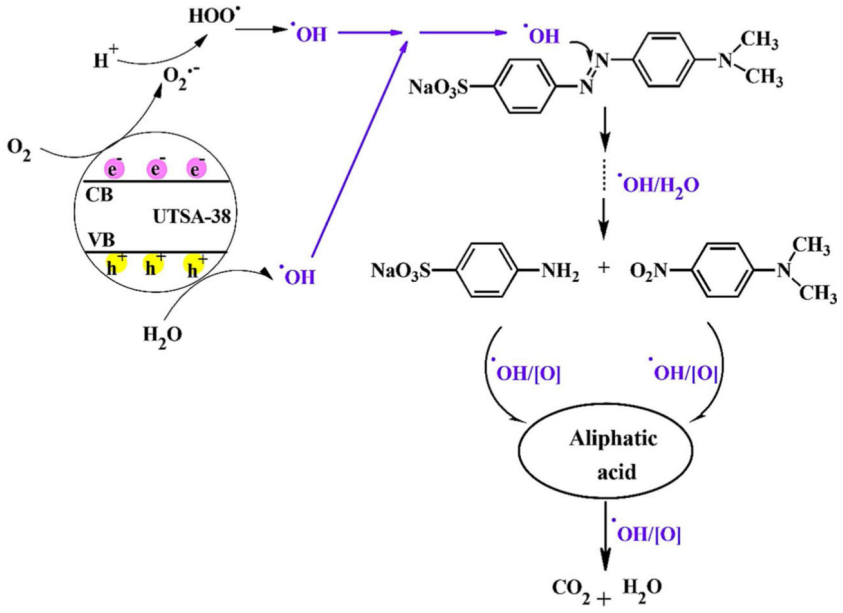

Fig. 12.

Main pathways proposed for the photodegradation of MO by UTSA-38 under visible or UV/vis light irradiation. Reproduced with permission from Ref (Das et al., 2011).

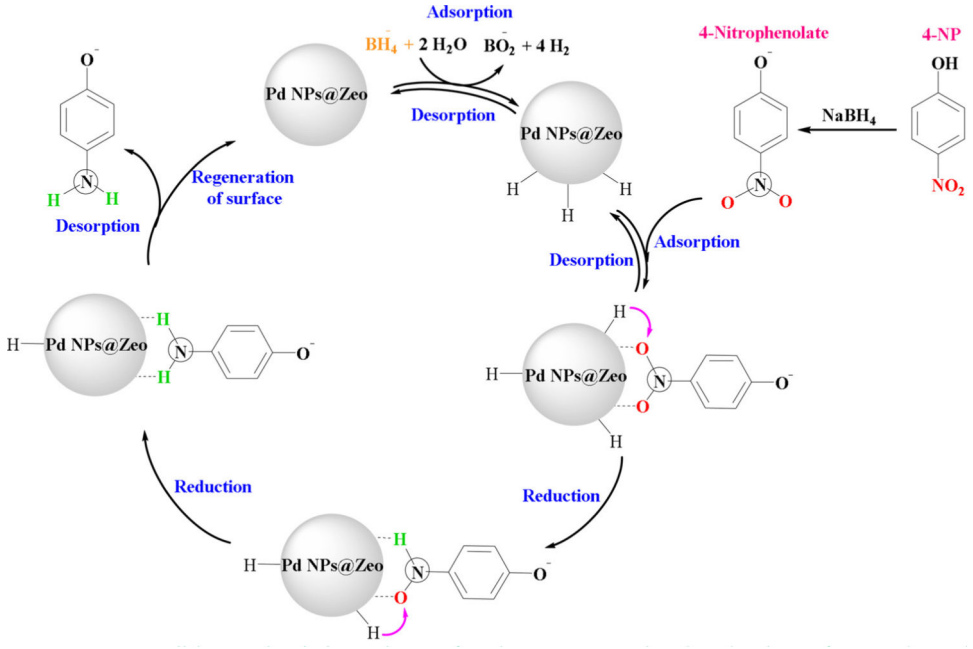

Fig. 13.

Possible mechanistic pathway for the $NaBH_4$-assisted reduction of 4-NP by Pd NPs@Zeo. Reproduced with permission from Ref (Nasrollahzadeh et al., 2020b).

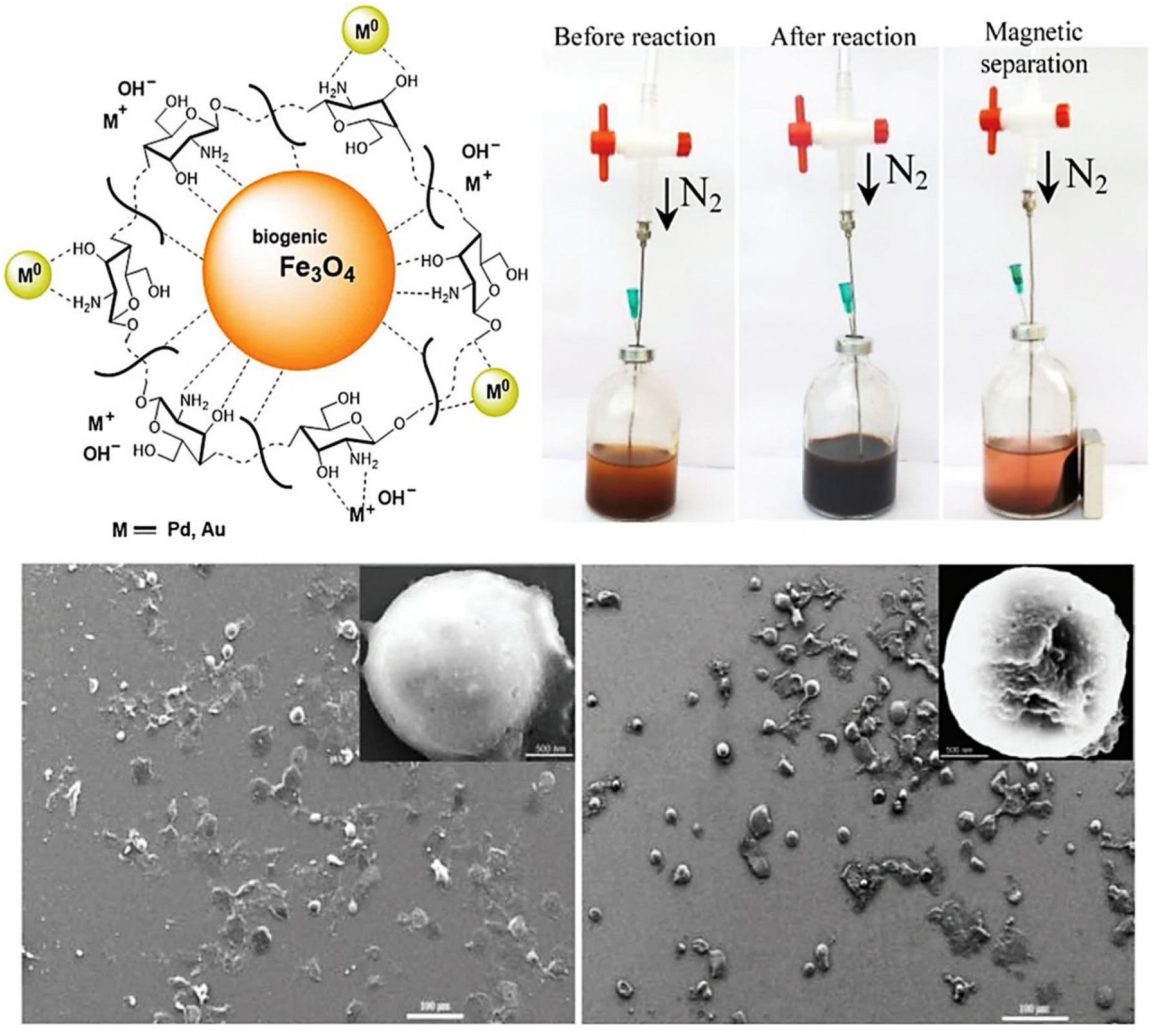

Fig. 14.

Biomolecule directed synthesis of a magnetite@chitosan-Au or Pd NPs and (HR)SEM images of well-dispersed spherically-shaped nanocomposite. Reproduced with permission from Ref (Parandhaman et al., 2016).

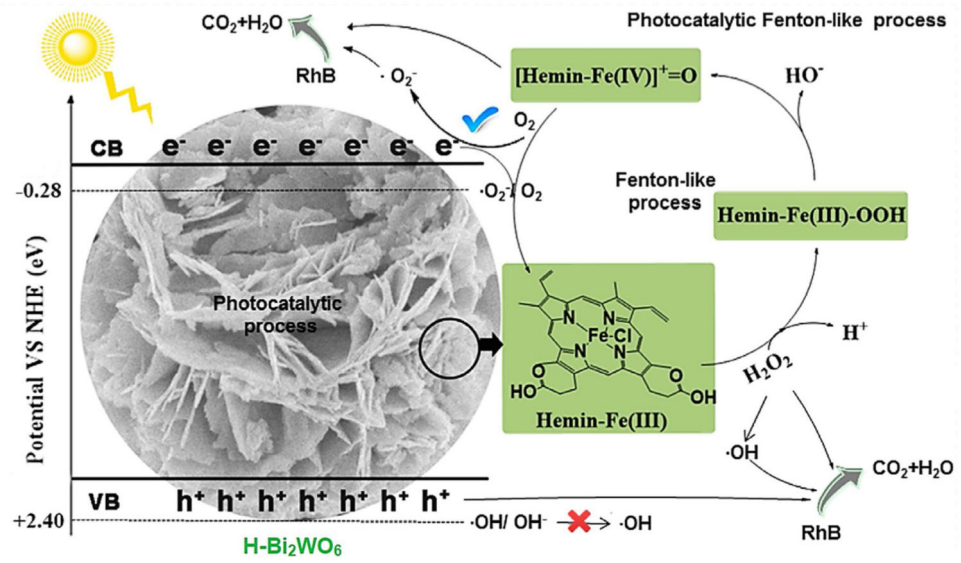

Fig. 15.

Proposed mechanism for the H_2O_2-assisted H-Bi_2WO_6 photocatalytic degradation of organic pollutants under solar irradiation. Reproduced with permission from Ref (Yi et al., 2018).

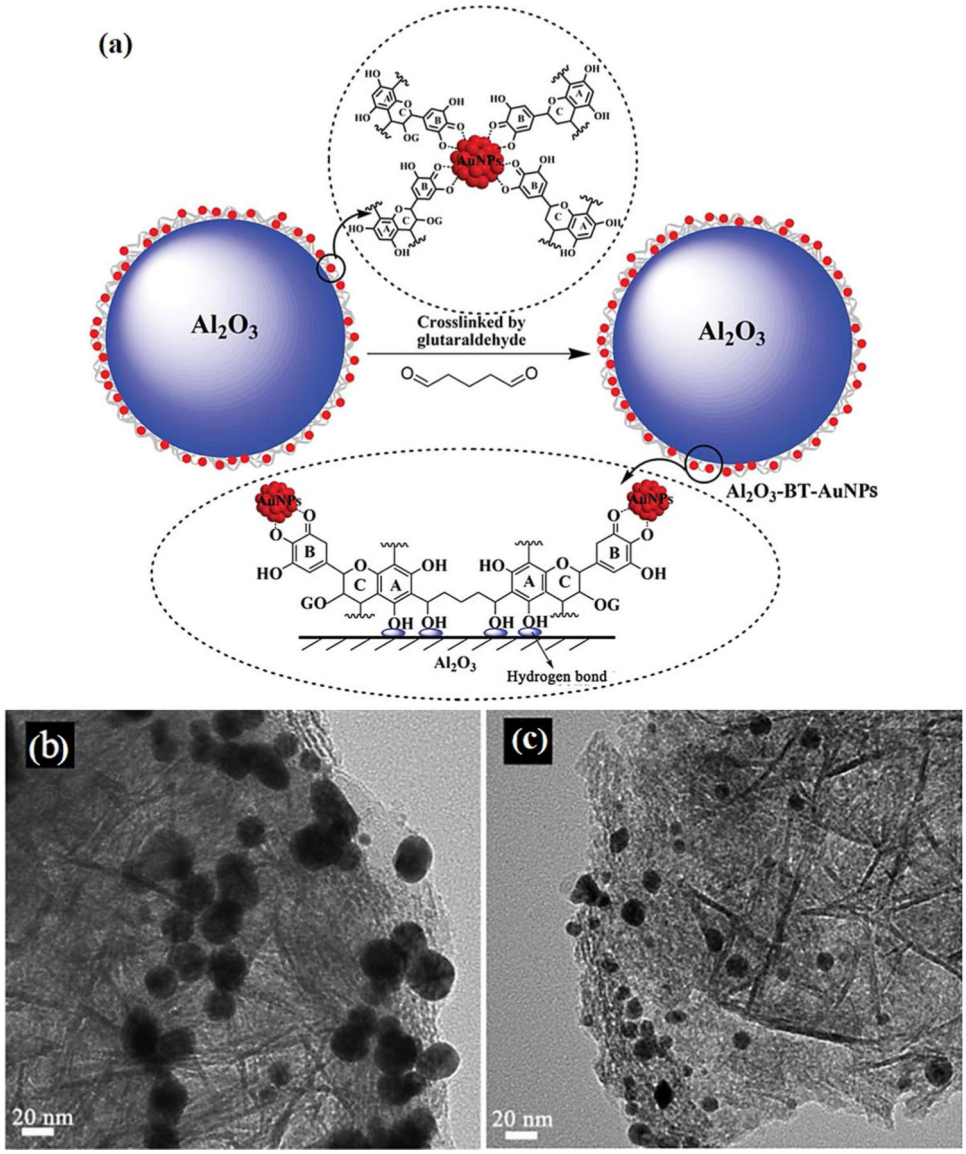

Fig. 16.

(a) Schematic diagram illustrating the biomolecule directed synthesis of Al_2O_3/BT/Au NPs, (b,c) (HR)TEM images of the well-dispersed spherically-shaped Au NPs on Al_2O_3 support. Reproduced with permission from Ref (Huang et al., 2011b).

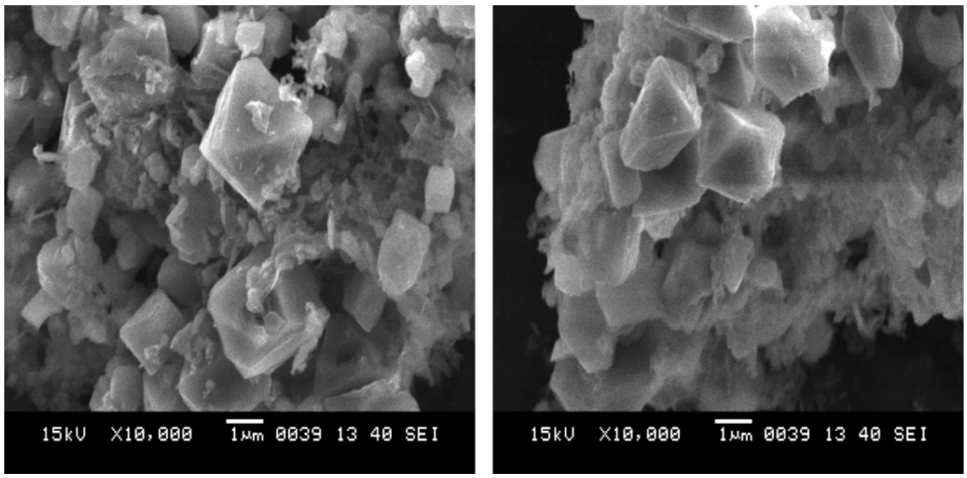

Fig. 17.

SEM images of the produced magnetic iron oxide NPs-Tea. Reproduced with permission from Ref (Lunge et al., 2014).

Fig. 18.

Green-produced iron oxide NPs dispersed onto zeolite by eucalyptus leaf extracts (EL-MNP@zeolite). Reproduced with permission from Ref (Xu et al., 2020).

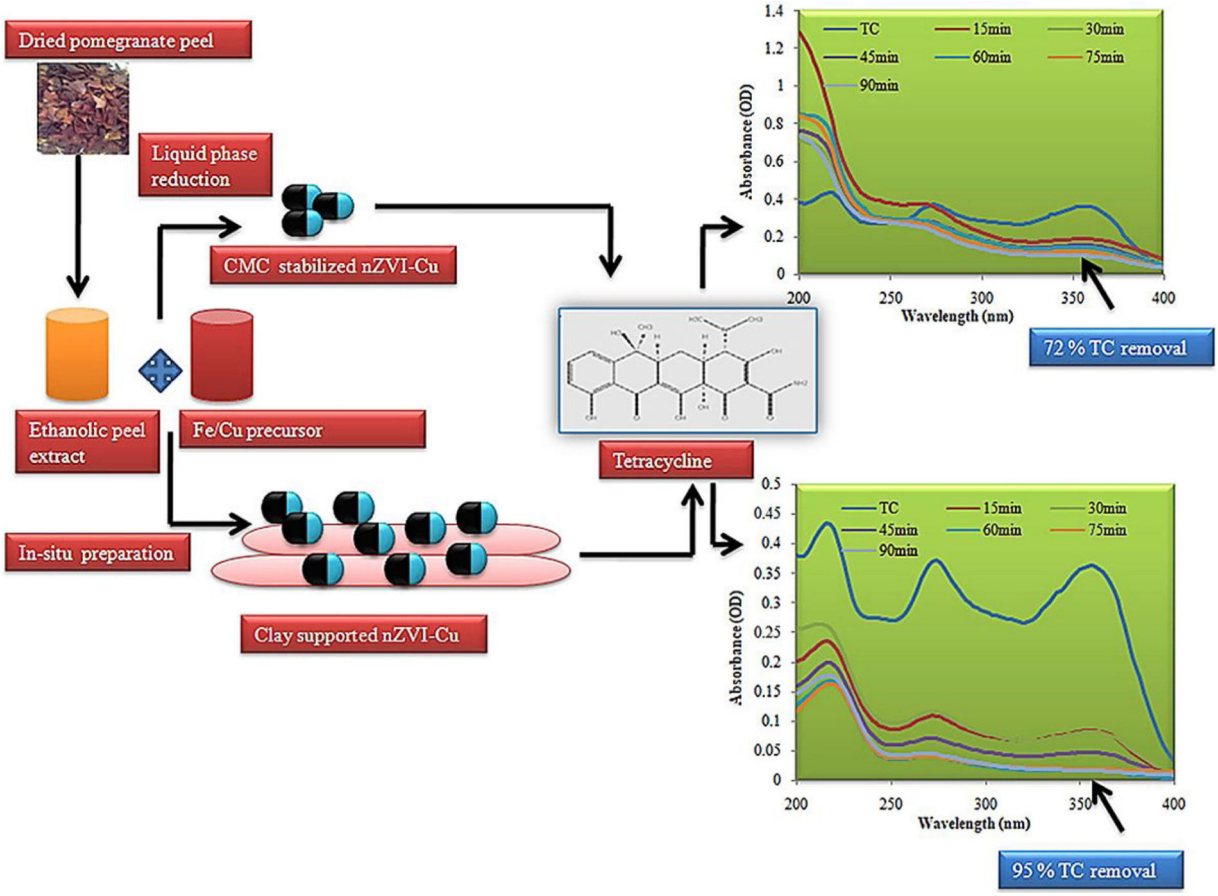

Fig. 19.

Bimetallic nZVI-Cu and bentonite supported green nZVI-Cu nanocomposite for removing tetracycline (TC). Reproduced with permission from Ref (Gopal et al., 2020).

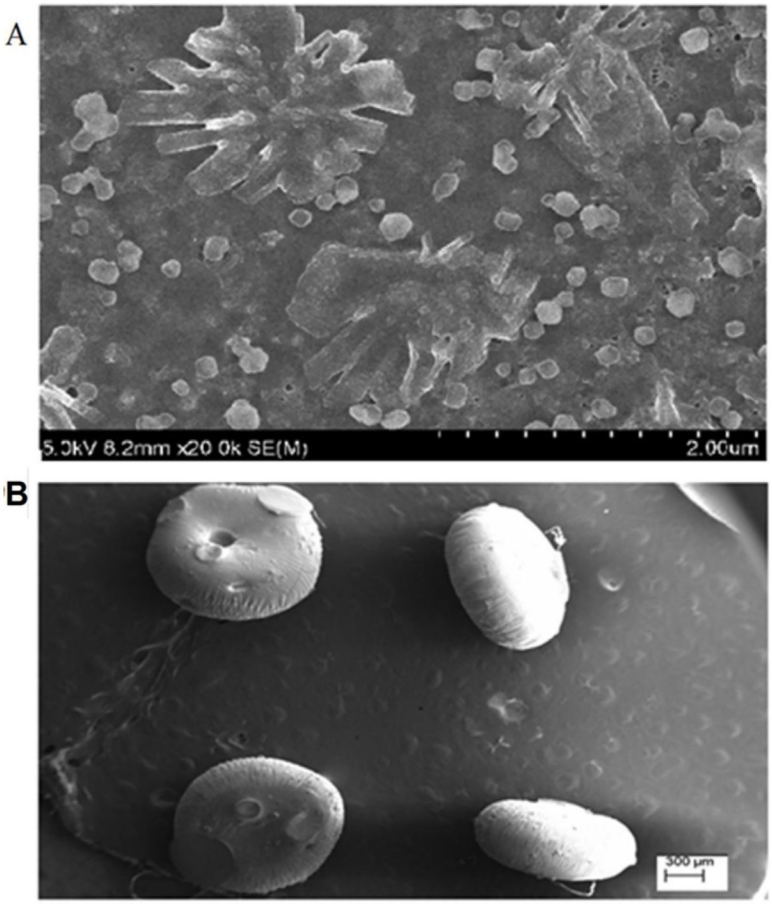

Fig. 20.

(A) SEM image of GS-NiFe NPs **(B)** SEM image of GS-NiFe beads. Reproduced with permission from Ref (Ravikumar et al., 2020).

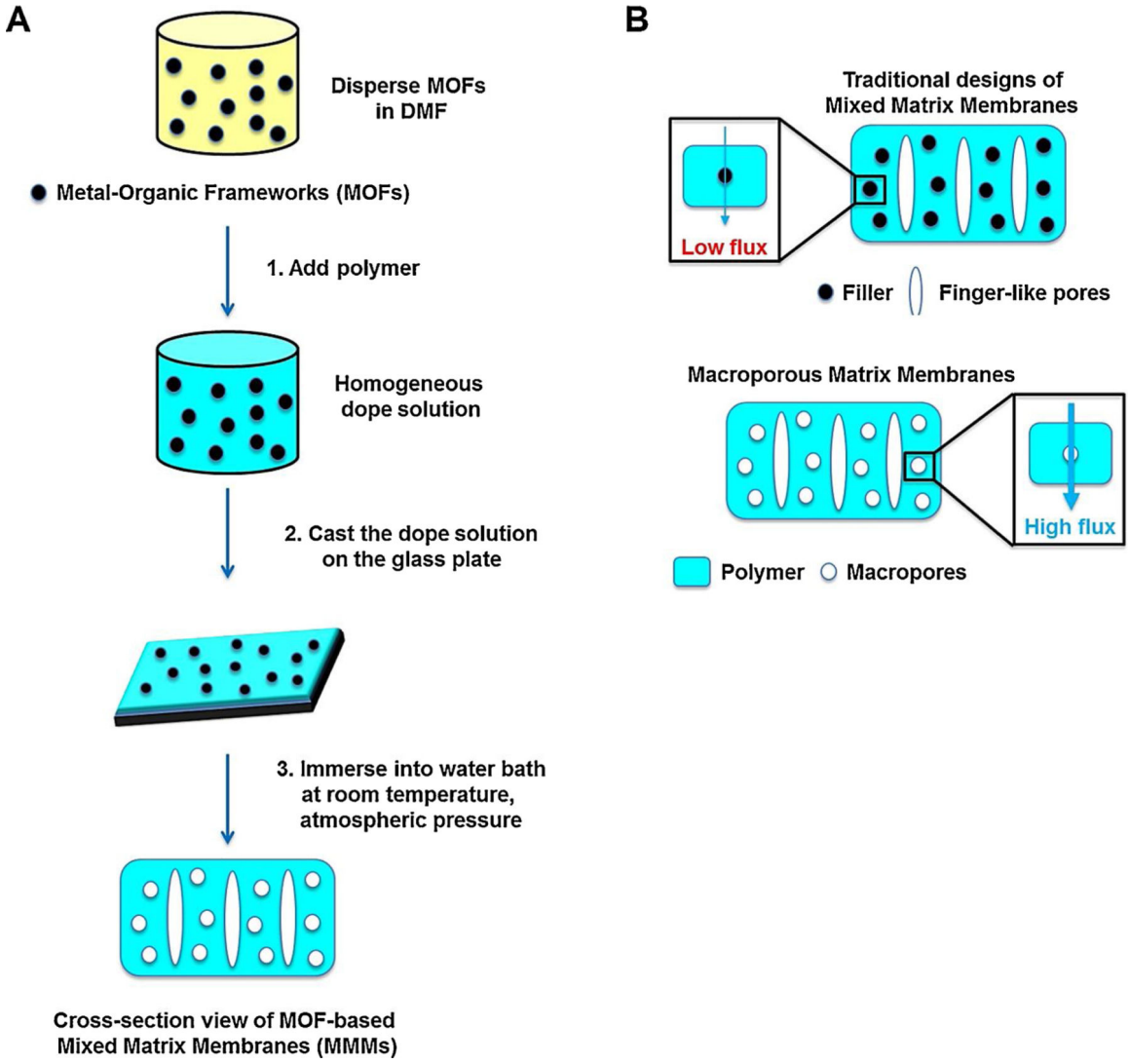

Fig. 21.

(A) PMMs fabrication strategy. (B) PMMs were fabricated by applying MOF as green template for treatment of water; the reported strategy was compared with traditional mixed matrix membranes. Reproduced (Adapted) with permission from Ref (Lee et al., 2014).

Table 1

Important biosynthesized metal and metal oxide-based nanocatalysts in the degradation of pollutants in water.

Entry	Nanocatalysts	Applications	Biogenic source	Refs.
1	Ag nanoparticles/clinoptilolite	Reduction of MB, MO, CR and RhB	*Vaccinium macrocarpon fruit*	(Khodadadi et al., 2017b)
2	rGO/Ag-Au NPs	Reduction of toxic Cr(VI)	*Albizia Saman* leaf	(Vellaichamy and Periakaruppan, 2016a)
3	Ag/zeolite nanocomposite	Reduction of MB, 4-NP, CR, RhB and MO	*Euphorbia prolifera* leaf	(Hatamifard et al., 2016)
4	AgPd NPs	Electrocatalytic reduction of H_2O_2	*Lithodora hispidula* (Sm.) Griseb. leaf	(Turunc et al., 2017)
5	Ag/RGO nanocomposite	Reduction of CR, 4-NP and RhB	*Abutilon hirtum* leaf	(Maryami et al., 2016)
6	ZnO-Ag nano custard apple	Degradation of MB	Pomegranate peel	(Kaviya and Prasad, 2015)
7	Ag/bentonite nanocomposite	Reduction of MB, 4-NP, CR and RhB	*Euphorbia larica*	(Sajadi et al., 2018)
8	Ag NPs	Photodegradation of bromo phenyl blue (BPB)	*Cirsium japonicum*	(Khan et al., 2016)
9	Ag-Mo/CuO NPs	Photodegradation of MB	*Azadirachta indica* leaf	(Rajendaran et al., 2019)
10	Au and Ag-Au NPs	Degradation of malachite green	*Bacillus safensis*	(Ojo et al., 2016)
11	Ag-SnO_2 nanocomposites	Degradation of MB, Methyl Violet 6B, Rose Bengal and 4-NP	*Saccharum officinarum*	(Sinha et al., 2017)
12	Ag@AgCl NPs	Degradation of Victoria Blue B	*Aquilaria agallocha* (AA) leaf juice	(Devi et al., 2016)
13	RGO nanosponge/Ag-NP	Reduction of 4-NP	*Tabebuia berteroi* leaf	(Vellaichamy and Periakaruppan, 2016b)
14	Ag NPs	Degradation of RB-21, reactive Red-141 (RR-141) and Rhodamine-6G	Palm shell	(Vanaamudan et al., 2016)
15	Ag NPs	Reduction of 4-NP	*Phoenix Dactylifera L. (date palm)* leaf	(Aitenneite et al., 2016)
16	Ag-ZnO	Photodegradation of MB	*Azadirachta indica* (Neem) leaf	(Patil et al., 2016)
17	Ag/MgO nanocomposite	Reduction of MB, 4-NP, MO and 2,4-dinitrophenylhydrazine (2,4-DNPH)	*Acalypha hispida*	(Nasrollahzadeh et al., 2020c)
18	Ag nanocomposite hydrogels based on sodium alginate	Removal of MB	*Mukia maderaspatna* leaf	(Karthiga Devi et al., 2016)
19	Ag/polyphenols-modified graphene	Reduction of 4-NP	Green tea	(Wang et al., 2015)
20	Ag/ZnO in montmorillonite	Photodegradation of MB	Urtica dioica leaf	(Sohrabnezhad and Seifi, 2016)
21	Ag NPs	Reduction of 4-NP	*Coleus forskohlii* root	(Naraginti and Sivakumar, 2014)
22	Ag/TiO_2 NPs	Photodegradation of MB	Rambutan (*Nephelium lappaceum* L.) peel	(Kumar et al., 2016a)
23	Ag-TiO_2 nanopowders	Photodegradation of MB	*Carambola*	(Chowdhury et al., 2016)
24	Ag NPs	Degradation of malachite green	Extract of paper wasp (*Polistes sp*)	(Lateef et al., 2016)
25	Ag NPs	Degradation of RhB and MB	*Parkia roxburghii* leaf	(Paul et al., 2016)

Entry	Nanocatalysts	Applications	Biogenic source	Refs.
26	Ag/AgCl NPs	Photodegradation of malachite green	*Benincasa hispida* (*ash gourd*) peel	(Devi and Ahmaruzzaman, 2016)
27	Ag NPs	Photodegradation of Putnam sky blue 39	*Rosa* 'Andeli' double delight petals aqueous extract (PERA)	(Suárez-Cerda et al., 2015)
28	Ag NPs/peach kernel shell	Reduction of MB, 4-NP and MO	*Achillea millefolium* L.	(Khodadadi et al., 2017a)
29	Ag NPs	Biosorbent to treat industrial effluents	*Morinda Tinctoria* leaf	(Vennila and Prabha, 2015)
30	Ag NPs	Photodegradation of MB	*Polygonum minus*	(Ullah et al., 2017)
31	Ag NPs	Photodegradation of Methyl Red (MR)	*Piper pedicellatum* C.DC leaf	(Tamuly et al., 2014)
32	Ag-Cr-AC nanocomposites	Removal of binary dye system of Reactive Red (RR) and CV	*Azadirachta indica* leaf	(Saad et al., 2017)
33	Ag/CN-TiO_2@g-C_3N_4	Photodegradation of RhB	Bamboo leaf	(Jiang et al., 2014)
34	Ag/Hazelnut shell nanocomposite	Reduction of MO and CR	*Origanum vulgare* leaf	
35	Ag NPs	Photodegradation of Coomassie Brilliant Blue G-250	*Coccinia grandis* leaf	(Arunachalam et al., 2012)
36	Ag NPs	Degradation of MB	*Plectranthus amboinicus* leaf	(Zheng et al., 2017)
37	Ag NPs	Photodegradation of MB	*Biebersteinia multifida*	(Miri et al., 2018a)
38	Ag/Cu NPs	Degradation of toxic chlorpyrifos pesticide	*Carica papaya*	(Rosbero and Camacho, 2017)
39	Ag NPs	Photodegradation of MB	*Trichodesma indicum* leaf	(Kathiravan, 2018)
40	Au@Ag@AgCl core-double shell NPs	Reduction of 2,4,6-trinitro phenol and photodegradation of ibuprofen and clofibric acid	*Momordica Charantia* leaf	(Devi and Ahmaruzzaman, 2017)
41	Ag NPs	Photodegradation of MB	*Prosopis farcta* fruit	(Miri et al., 2018b)
42	Ag NWs-rGO nanosheets	Reduction of 4-NP and 2-nitrophenol (2-NP)	*Abelmoschus esculentus*	(Gnanaprakasam and Selvaraju, 2014)
43	Ag@Fe bimetallic NPs	Degradation of bromothymol blue	Palm dates fruit	(Al-Asfar et al., 2018)
44	Ag and Au NPs	Reduction of 4-nitroaniline	*Citrus aurantifolia* peel	(Dauthal and Mukhopadhyay, 2015)
45	Ag NPs	Reduction of EY and CR	*Synedrella nodiflora* leaf	(Vijayan et al., 2018)
46	Au-Ag bimetallic nanocomposite	Reduction of 4-NP	*Silybum marianum* seed	(Gopalakrishnan et al., 2015)
47	Ag NPs	Degradation of MB	*Trichodesma indicum* leaf	(Kathiravan, 2018)
48	Ag NPs	Reduction of 4-NP	lavender leaf	(Kumar et al., 2016b)
49	Ag NPs	Reduction of 4-NP, MB, MO and MR	*Stemona tuberosa Lour*	(Bonigala et al., 2018)
50	Ag/HZSM-5 nanocomposite	Reduction of MB, CR, RhB and 4-NP	*Euphorbia heterophylla* leaf	(Tajbakhsh et al., 2016)
51	Ag NPs	Reduction of 4-NP	*Ficus hispida* Linn. f. leaf	(Ramesh et al., 2018)
52	Ag NPs	Reduction of poisonous nitro compounds	Extract of date palm	(Farhadi et al., 2017)
53	Ag NPs	Degradation of CR and MO	*Salvia microphylla Kunth* leaf	(Lopez-Miranda et al., 2018)
54	Ag NPs	Reduction of Eosin Blue (EB) and 4-NP	*Sapindus mukorossi* fruit	(Dinda et al., 2017)
55	Ag NPs	Reduction of 4-NP	Citrus maxima peel	(Huo et al., 2018)

Entry	Nanocatalysts	Applications	Biogenic source	Refs.
56	Ag NPs/almond shell	Reduction of MB, RhB and 4-NP	*Ruta graveolens* sleeves	(Bordbar, 2017)
57	Ag NPs	Reduction of 4-NP	*Allium ampeloprasum* L. leaf	(Khoshnamvand et al., 2019)
58	Au, Ag and Ag/Au alloy NPs	Reduction of 4-NP	*Guazuma ulmifolia* L. bark	(Karthika et al., 2017)
59	Ag NPs	Photodegradation of MB	Mortiño berry	(Kumar et al., 2019)
60	Pd NPs	Reduction of 4-NP	Frimiana simplex	(Peng et al., 2019)
61	Pd NPs	Reduction of organic pollutant	*Lagerstroemia speciosa*	(Garole et al., 2019)
62	Natrolite zeolite/Pd nanocomposite	Reduction of MB, MO, CR, RhB and 4-NP	*Piper longum* fruit	(Hatamifard et al., 2015)
63	Pd-RGO nanocomposite	Degradation of dye pollutants	*Rosa Canina fruit*	(Nasrollahzadeh et al., 2020d)
64	Au-Pd	Reduction of 3-nitroaniline	*Delonix regia*	(Dauthal and Mukhopadhyay, 2016)
65	Pd NPs	Reduction of dyes	*Anogeissus latifolia* gum	(Kora and Rastogi, 2018)
66	Pd NPs	Degradation of Bismarck brown and antidandruff	*Lagenaria siceraria*	(Kalpana and Rajeswari, 2018)
67	Pd NPs	Photodegradation of MB	*Andean blackberry*	(Kumar et al., 2015)
68	Pd NPs	Cr(VI) reduction	*Garcinia pedunculata* Roxb	(Hazarika et al., 2017)
69	Pd NPs	Reduction of organic dyes	*Terminalia arjuna*	(Garai et al., 2018)
70	Pd/RGO	Reduction of various dyes	*Artemisia abrotanum*	(Hashemi Salehi et al., 2019)
71	Pd/perlite nanocomposite	Reduction of 4-NP, CR, RhB, MO and 2,4-DNPH	*Euphorbia neriifolia* L. leaf	(Maryami et al., 2017)
72	Pd NPs	Degradation of dyes	*Pimpinella tirupatiensis*	(Narasaiah et al., 2017)
73	Pd/walnut shell nanocomposite	Degradation of RhB, CR, and MB	*Equisetum arvense* L.	(Bordbar and Mortazavimanesh, 2017)
74	Pd/Fe_3O_4 nanocomposite	Degradation of Cr(VI), 4-NP and 2,4-DNPH	*Hibiscus tiliaceus* L.	(Nasrollahzadeh et al., 2018b)
75	Pd/bentonite nanocomposite	Degradation of 2,4-DNPH, Cr(VI), and 4-NP	*Gardenia taitensis* leaf	(Nasrollahzadeh et al., 2018c)
76	Pd NPs/sodium borosilicate glass	Reduction of 4-NP, 2,4-DNPH, MO, CR, MB, and Cr(VI)	*Euphorbia milii*	(Nasrollahzadeh et al., 2018d)
77	Pd NPs	Diatrizoate removal from hospital wastewater	*S. oneidensis*	(De Gusseme et al., 2011)
78	Cu/reduced graphene oxide/Fe_3O_4 nanocomposite	Reduction of 4-NP and RhB	*Euphorbia wallichii* leaf	(Atarod et al., 2015)
79	CuO/ZnO nanocomposite	Reduction of 4-NP and RhB	*Melissa Officinalis* L. leaf	(Bordbar et al., 2018)
80	Cu NPs	Degradation of MR	Peel extract of *Citrus grandis*	(Sinha and Ahmaruzzaman, 2015)
81	CuO NPs	Photodegradation of MB	*Tinospora cordifolia*	(Nethravathi et al., 2015)
82	Cu/ZnO NPs	Degradation of MB and CR	*Euphorbia prolifera* leaf	(Momeni et al., 2016)
83	Cu NPs	Degradation of Bismarck brown	*Tridax procumbens* leaf	(Kalpana et al., 2016)
84	Cu nanoflowers	Degradation of MB	*Ficus benghalensis* leaf	(Robati et al., 2016)
85	CuO NPs	Reduction of 4-NP	*Tecoma castanifolia* leaf	(Sharmila et al., 2016)

Entry	Nanocatalysts	Applications	Biogenic source	Refs.
86	Cu/Fe_3O_4/eggshell nanocomposite	Reduction of MO, 4-NP, CR, RhB and MB	*Orchis mascula* L. leaf	(Nasrollahzadeh et al., 2016a)
87	Cu/Fe_3O_4 NPs	Reduction of 4-NP, CR and RhB	*Morinda morindoides* seeds	(Nasrollahzadeh et al., 2016b)
88	CuO nanocrystals	Degradation of MB, MO, MR, EY and reduction of 2-NP, 3-NP and 4-NP	*Psidium guajava* leaf	(Sreeju et al., 2017)
89	CuO NPs	Reduction of 4-NP	Fruit extract of plant *Fortunella japonica*	(Singh et al., 2017)
90	CuO NPs	Photodegradation of Acid Black 210 (AB)	*Abutilon indicum*	(Ijaz et al., 2017)
91	CuO NPs	Degradation of 4-NP	Rosehip	(Jafarirad et al., 2018)
92	CuO NPs	Reduction of CR, MB and 4-NP	*Aglaia elaeagnoidea* flowers	(Manjari et al., 2017)
93	CuO NPs	Photodegradation of RhB	*Ferulago angulata (schlecht) boiss*	(Mehr et al., 2018)
94	CuS NPs	Degradation of safranin O (SO)	*Calotropis gigantean* leaf	(Ayodhya and Veerabhadram, 2017)
95	CuO NPs/clinoptilolite	Degradation of 4-NP, RhB and MB	*Rheum palmatum* L. root	(Bordbar et al., 2017)
96	Cu-doped ZnO NPs	Degradation of Acid Black 234	*Clerodendrum infortunatum* and *Clerodendrum inerme*	(Khan et al., 2018)
97	Cu NPs	Removal of nitrate	Extract of *Hibiscus sabdariffa* flowers	(Paixão et al., 2018)
98	CdS	Removal of Cd	*P. aeruginosa* JP-11	(Raj et al., 2016)
99	Se	Removal of Zn(II)	Anaerobic microbial consortium	(Jain et al., 2015)
100	Se	Removal of Hg^0	*Citrobacter freundii* Y9	(Wang et al., 2018)
101	Mn	Removal of Pb(II), Cd(II), and Zn(II)	*Pseudomonas putida MnB1*	(Zhou et al., 2015)
102	MgO	Removal of Ni(II),Pb(II) Cd(II), Cu(II), Zn(II),Co(II), Mn (II)	*Acacia* sp.	(Srivastava et al., 2015)
103	ZnO NPs	Degradation of Synozol Navy Blue-KBF textile dye	*Trianthema portulacastrum*	(Khan et al., 2019)
104	ZnO nano-flowers	Photodegradation of MB, EY and Malachite green (MG)	Panos	(Kaliraj et al., 2019)
105	ZnO NPs	Degradation of CR	*Artocarpus Heterophyllus* leaf	(Vidya et al., 2017)
106	ZnO NPs	Degradation of Alizarin Red-S	*Carica papaya* milk (CPM) latex	(Sharma, 2016)
107	ZnO NPs	Photodegradation of MB	*Hydnocarpus alpina* Wt	(Ganesh et al., 2019)
108	SnO_2-ZnO	Degradation of MO	Gel of *Aloe vera* plant	(Sudhaparimala and Vaishnavi, 2016)
109	ZnO NPs	Degradation of RhB and MB	Seeds extract of *Parkia roxburghii*	(Paul et al., 2017)
110	ZnO/MgO nanocomposite	Degradation of MO, MB and 2-NP	*Musa paradisiaca* bract	(Maruthai et al., 2018)
111	ZnO/$NiFe_2O_4$ NPs	Photodegradation of MB	*Mangifera indica* leaves	(Adeleke et al., 2018)
112	ZnO NPs	Photodegradation of RhB	*Cyanometra ramiflora* leaf	(Varadavenkatesan et al., 2019)
113	ZnO NPs	Photodegradation of MB	*Thymus vulgaris* leaf	(Zare et al., 2019)
114	ZnO NPs	Degradation of MO, CR, RhB and MB	*Abelmoschus esculentus* mucilage	(Prasad et al., 2019)
115	Fe-ZnO NPs	Photodegradation of naphthalene	*Amaranthus dubius* aqueous leaf	(Muthukumar et al., 2017)

Entry	Nanocatalysts	Applications	Biogenic source	Refs.
116	ZrO_2/rGO nanocomposite	Photodegradation of RB 4 dye	Cinnamon	(Gurushantha et al., 2017)
117	Hollow microspheres Mg-doped ZrO_2 NPs	Photodegradation of RhB	*Aloe vera* gel	(Renuka et al., 2016)
118	rGO/TiO_2/Co_3O_4	Degradation of MB and CV	*Shuteria involucrata* leaf	(Ranjith et al., 2019)
119	α-Fe_2O_3/TiO_2	Degradation of MB	Flax seed	(Mohamed et al., 2019)
120	SnO_2 NPs	Photodegradation of MB, MO and erichrome black T	*Erwinia herbicola*	(Srivastava and Mukhopadhyay, 2014)
121	Au NPs	Reduction of 4-NP	*Trichoderma viride* and *Hypocrea lixii*	(Mishra et al., 2014)
122	Au NPs	Degradation of CR and MB	Cellular extract of *Bacillus marisflavi*	(Nadaf and Kanase, 2016)
123	Au NPs	decolorization of cationic Red X-GRL, Acid Orange II and Acid scarlet GR	*Aspergillum* sp. WL-Au	(Qu et al., 2017)
124	Au NPs	Reduction of 4-NP	*Aspergillum* sp. WL-Au	(Shen et al., 2017)
125	Manganese oxides	Removal of bisphenol A	*Desmodesmus* sp. WR1	(Wang et al., 2017)
126	nano-MnO_x	Oxidative degradation of 2-chlorophenol, 2,4-dichlorophenol, and 2,4,6-trichlorophenol	*Pseudomonas* sp. G7	(Tu et al., 2015)
127	$Dy_2Ce_2O_7$ nanostructure	Degradation of MO, and RhB and B nepthol	*Vitis vinifera* juice	(Zinatloo-Ajabshir et al., 2018a)
128	$Ln_2Sn_2O_7$ nanostructure	Degradation of EY, eriochrome black T and methyl violet	*Pomegranate* juice	(Zinatloo-Ajabshir et al., 2018b)
129	Bio-Pt and bio-Pd nanocatlyst	Removal of ciprofloxacin, sulfamethoxazole and 17b-estradiol	*Desulfovibrio vulgaris*	(Martins et al., 2017)
130	Pd/Au	Dechlorination of diclofenac	*Shewanella oneidensis* MR-1	(De Corte et al., 2012)

J Hazard Mater. Author manuscript; available in PMC 2022 January 05.

Table 2

Appliances of biogenic iron-based NPs in degradation of dyes and removal of heavy metals.

Entry	Biogenic source	Nanoparticle size & shape	Dye/metal removed	Refs.
1	*Eucalyptus*	20–80 nm, spherical	Swine wastewater treatment	(Wang et al., 2014a)
2	*Mentha spicata*	20–45 nm, core and shell morphology	As(III) & As(V)	(Prasad et al., 2014)
3	*Sorghum bran*	40–50 nm, amorphous	Bromothymol blue	(Njagi et al., 2010)
4	Green, Oolong and Black tea	20–40 nm, spherical	Monochlorobenzene	(Kuang et al., 2013)
5	*Amaranthus dubis*	60–300 nm, spherical	MO	(Harshiny et al., 2015)
6	*Eucalyptus tereticornis, Melaleuca nesophila, Rosmarinus officinalis*	40–60 nm, spherical	Azo dye	(Wang et al., 2014b)
7	Black tea	40–50 nm	Ametryn	(Ali et al., 2016)
8	*Oak, mulberry* and cherry	10–30 nm, spherical	As(III) & Cr(VI)	(Poguberović et al., 2016)
9	*Amaranthus spinosus*	58–530 nm, spherical	MB, MO	(Muthukumar and Matheswaran, 2015)
10	*Eucalyptus*	20–60 nm, spherical agglomerates	Direct black G	(Zhuang et al., 2015)
11	*Omani* leaf	15 ± 2 in length and 3.0 ± 0.2 nm dia, nanorod	Heavy oil viscosity treatment	(Al-Ruqeishi et al., 2016)
12	*Aloe vera*	100 × 20 nm, nanorod	As(V)	(Mukherjee et al., 2016)
13	Black tea	40–50 nm, spherical	Fluoride	(Ali et al., 2015)
14	*Phyllanthus acidius*	4.5–5.8 nm, spherical	AO7	(Gurushantha et al., 2015)
15	*Grape* leaf	10–100 nm, quasi spherical shape	Orange II dye	(Luo et al., 2016)
16	*Eichhornia crassipes* (water hyacinth)	20–80 nm, amorphous	Cr(VI)	(Wei et al., 2017)
17	*Eucalyptus* leaf	20 and 80 nm, amorphous	Cr(VI), Cu(II)	(Weng et al., 2016)
18	Green tea	5–15 nm, spherical	Bromothymol blue	(Hoag et al., 2009)
19	*Eucalyptus*	50–80 nm, spherical	Cr(VI)	(Madhavi et al., 2013)
20	*Eucalyptus*	40–60 nm, amorphous	Acid black 194	(Wang, 2013)
21	Green, Oolong and Black tea	40–50 nm, spherical	Malachite green	(Huang et al., 2014a)
22	*Pomegranate*	100–200 nm	Cr(VI)	(Rao et al., 2013)
23	*Vine* leaves, black tea, *grape marc*	15–45 nm	Ibuprofen	(Machado et al., 2013)
24	*E. globules*	80–90 nm, spherical	Phosphate	(Gan et al., 2018)
25	*E. globules*	~80, spherical	Nitrate	(Wang et al., 2014c)
26	*Aloe vera*	5.5, Rod like	As(V)	(Mukherjee et al., 2016)
27	*M. oleifera*	250–474, spherical	Nitrate	(Katata-Seru et al., 2018)
28	*C. sinensis*	5–25, Cuboid/Pyramidal	As(V) & As(III)	(Lunge et al., 2014)

Entry	Biogenic source	Nanoparticle size & shape	Dye/metal removed	Refs.
29	*M. ferrooxydans*	100–130, Rope like	As(III) & As(V)	(Andjelkovic et al., 2017)
30	*E. globules*	-, spherical	As(V)	(Martínez-Cabanas et al., 2016)
31	*C. reticulata*	~50, spherical	Cd(II)	(Ehrampoush et al., 2015)
32	*S. thermolineatus*	25, distorted spherical	Cu	(Kandasamy, 2017)
33	*S. jambos*	5–60, Oval, spherical	Cr(VI)	(Xiao et al., 2016)
34	*E. globules*	50–80, spherical	Cr(VI)	(Madhavi et al., 2013)
35	*P. granatum*	100–200, irregular	Cr(VI)	(Rao et al., 2013)
36	*C. sinensis, S. aromaticum, M. spicata, P. granatum*	50–60, spherical	Cr(VI)	(Mystrioti et al., 2016)
37	*C. (L.) Cuss*	~45.4, irregular	Cr(III) & Pb(II)	(Lingamdinne et al., 2017)
38	Oolong tea	40–50 nm, spherical	Malachite green	(Huang et al., 2014b)
39	Green tea	70–80 nm, spherical	Malachite green	(Huang et al., 2015)
40	*Eucalyptus* leaf	80 nm, spherical	Phosphate	(Cao et al., 2016)